Diagnosis of Industrial Catalyst Deactivation by Surface Characterization Techniques

P. Govind Menon*

Laboratorium voor Petrochemische Techniek, Universiteit Gent, Krijgslaan 281, B-9000 Gent, Belgium, and Department of Engineering Chemistry, Chalmers University of Technology, S-41296 Göteborg, Sweden

Received November 4, 1993 (Revised Manuscript Received March 30, 1994)

Contents

I. Introduction

Heterogeneous catalysis is basically a surface phenomenon. Hence a knowledge of the exact chemical composition of the surface is a primary requisite for understanding the working of solid catalysts. Whether or not the actual surface composition of a catalyst is the same as its bulk composition has remained a basic question in catalysis for the last 60 years or more. Until recently, there was hardly any experimental technique which could give an unambiguous answer to this question. But, more than a century ago, it was predicted by Willard Gibbs[1] that the equilibrium composition of an alloy surface might not necessarily be its bulk composition and that one of the components could segregate or be enriched on its surface. With the advent of modern experimental techniques for surface analysis, the elemental composition of the surface layer (up to a few atomic layers) can be determined more or less quantitatively. This is a tremendous advance over the situation of the preceding 3 or 4 decades when specific chemisorption of gases was practically the only method available to probe the chemical nature of the surface layer of a heterogeneous catalyst.

Many of the recent studies in this area show that the composition of the catalyst surface in many cases can be quite different from that of the bulk. More interesting for catalysis, however, are the changes occurring in the chemical composition of the surface *during* pretreatments (like calcination, reduction, or sulfiding) of the catalyst and *as a consequence* of the catalytic reaction itself on it. This suggests that the predominant species observed on the surface of a fresh catalyst in its virgin state may not even be the active species at all under actual reaction conditions. In this respect, investigations on used or equilibrium catalysts will be more relevant than those on the fresh ones, provided the former can be handled under conditions which do not change them further (e.g., exposure of reduced metallic catalysts to air may reoxidize them). The changes from a fresh to a used catalyst may also reveal how a catalyst is activated and also deactivated in the course of time.

Surface enrichment phenomena have been studied most extensively on alloy catalyst systems, which have been reviewed comprehensively by Overbury et al.,[2] Ponec,[3] Sachtler,[4] Sachtler and van Santen,[5] and Somorjai.[6] Hence alloy catalysts will not be discussed

* Please address correspondence to the author at his Universiteit Gent address.

0009-2665/94/0794-1021$14.00/0

Govind Menon received his M.Sc. and M.Tech. degrees in India from Banaras Hindu University and Indian Institute of Technology, Kharagpur, respectively. His Ph.D. work on "adsorption of N_2 and CO on alumina up to 3000 bar pressure" was carried out under the supervision of Prof. A. Michels at the Van der Waals Laboratory, University of Amsterdam, and the thesis was written under the guidance of Prof. J. H. de Boer (1961, Technological University, Delft, The Netherlands). A postdoctoral year as a Humboldt Fellow was spent with Prof. W. Jost at Göttingen. Half of Menon's subsequent career in catalysis research and development was spent in industry (Akzo-Ketjen; Indian Petrochemicals Corp. as Manager of Research and Development; and Dow Chemical, in the Netherlands) and the other half in academia (Regional Research Laboratory, Hyderabad, India; University of Gent in Belgium; and Chalmers University of Technology, in Sweden). A time-sharing of 80%–20% between Dow Chemical in the Netherlands and Chalmers University in Sweden for 6 years (1984–90) deserves special mention. Other activities include several lecture tours in India, Benelux, Sweden, United States, and Canada, industrial consulting, writing popular-science articles, and as Chairman of Catalyst Research Committee of the Council of Scientific & Industrial Research of India in 1974–77 and Catalysis Specialist on assignments of United Nations Development Program. He is interested equally in both the applied and fundamental aspects of industrial catalysis. His work in recent years was on catalysts for catalytic cracking, reforming, ammoxidation, selective hydrogenation, catalytic combustion, hydrogen effects in catalysis, UHV/molecular-beam studies on loss of alkali promoter from industrial catalysts for styrene, steam reforming, and ammonia synthesis, to name a few. At present he is Research Professor (part-time) of Industrial Catalysis in Sweden, both at Chalmers University of Technology, Göteborg, and Royal Institute of Technology, Stockholm, but he works the major part of his time (sponsored partly by Dow Chemical) at the Laboratorium voor Petrochemische Techniek of the University of Gent in Belgium and lives across the border at Terneuzen in the Netherlands.

any further in this review unless they are of direct interest in an industrial catalytic process. The scope of this review is restricted to surface enrichment or depletion in metal–oxide and supported-metal catalyst systems, as commonly used in industry. This area was last reviewed in 1979 by Menon and Prasada Rao.[7]

A. Experimental Methods for Characterization of Solid Catalysts

There are several excellent text books, monographs, and reviews on the various experimental techniques which are used routinely or occasionally for characterization of solid catalysts. Some of these (only a very small selection) are given in refs 8–11. State-of-the-art reviews on the experimental techniques and their applications in catalysis have also appeared from time to time in the numerous volumes of *Advances in Catalysis* and *Catalysis Reviews—Science & Engineering*. Shorter descriptions of only the principles of the techniques, without much theoretical background or experimental details, can be seen in books, for instance, by Srivastava,[12] by Brongersma and van Santen,[13] and very recently by Wachs[14] and by Niemantsverdriet.[15] Three of the five chapters in Volume 9 of the Specialist Periodical Reports entitled *Catalysis*[16] are devoted to catalyst deactivation, troubleshooting, and characterization of deactivated catalysts. A comprehensive bibliography for "Catalyst Characterization" just for the two-year period from July 1984 to June 1986, published by Austermann et al.[17] in *Anal. Chem.*, contains 794 references to journal articles. That is an indication of the intensity of research work in this area at the present time.

It has to be emphasized here that, despite the development of several sophisticated and even unique (and expensive) surface-science techniques, the old or classical techniques like surface area, pore volume and pore-size distribution measurements by physical adsorption/desorption (and mercury porosimetry), specific metal dispersion by chemisorption, surface-gas titration and temperature programmed techniques, X-ray diffraction, scanning and transmission electron microscopy continue to be the main work-horses in many catalysis research laboratories. For studies of catalyst deactivation and poisoning in particular, specific chemisorption, either directly as such or in its modified form as in surface gas titration or temperature-programmed desorption (TPD) or in a more reactive form as in temperature-programmed reduction/oxidation/sulfiding/coke-combustion/reaction spectroscopy (TPR/TPO/TPS/TPCC/TPRS), continues to be invaluable for characterizing fresh and used catalyst surfaces. These techniques provide not only a measure of the total metal and individual metal dispersions but also valuable information on the extent and type of metal-support interaction, cluster or alloy formation, the role of promoters, oxidation states of the metal on the surface, surface enrichment/depletion of a particular component, spillover phenomena, availability of selective and nonselective lattice oxygen in an oxide catalyst, location of coke on a deactivated catalyst (on the metal or on the support?), etc. Such applications have been reviewed earlier by Menon.[18] The distinctive advantages of the surface-titration technique are the relatively simple and self-made equipment, much lower cost, and quicker measurements, which bring this technique within the reach of practically any catalysis laboratory today. Its disadvantages are the lack of specificity of chemisorption in some cases, the complexity due to different forms of chemisorption, surface enrichment sometimes caused by chemisorption itself, slow or time-dependent chemisorption, and strong metal-support interaction (SMSI), to name a few. Fortunately, one can often recognize these limitations as peculiarities of the catalyst-adsorbate system and hence resort to other complementary techniques. Except in such restricted cases, a wealth of information can be obtained from chemisorption on and/or reactive gas titration of composite catalyst surfaces.

In view of the ready availability and accessibility of the theoretical background and experimental details of the various techniques for catalyst characterization, as indicated above, these aspects will not be covered in the present review. The *applications* of these techniques, often in a concerted and complementary way

for trouble-shooting on industrial catalysts, when something goes wrong with them, is the main theme to be dealt with here. Such information is often scattered in the literature; much of it is not even published due to secrecy considerations in industrial research and development (R&D). On the other hand, researchers in applied catalysis have occasionally to deal with "mysterious" cases of catalyst deactivation. Examples of earlier case histories of such deactivation phenomena can then be a practical guide for trouble-shooting. This is indeed one of the primary goals of this review.

B. Scope of the Review

As pointed out in the Introduction and later in section II, the exact nature of the catalyst surface and the various ways of catalyst deactivation are subjects of great scientific interest and enormous economic importance. Hence international catalysis conferences have been devoted to these topics every 3–4 years for the last few decades. A brief review like the present one has to be very selective, giving only the underlying principles and representative examples. It cannot be comprehensive; there is no need for it either.

The focus of this review is on industrial catalysts, in particular, on the most commonly used supported metal and mixed-oxide type catalysts. Here again, only typical examples are chosen and cited to illustrate the specific types of problems involved in catalyst deactivation and how these problems were diagnosed by a judicious application of the experimental techniques available today. Comparative studies of fresh, used, and deactivated or spent catalysts are most instructive. The rewards of such studies could be four-fold: (a) pinpoint the exact causes for catalyst deactivation, (b) suggest methods to reduce or prevent such deactivation, (c) lead to substantially improved process in the already existing plant, and (d) sometimes show the way to the design of still better industrial catalysts. Many examples for these are cited under III. Case Histories. Of these, examples H (fluid catalytic cracking catalyst), I (styrene catalyst), O (Ru catalyst for glucose hydrogenation), and Z (high-temperature catalytic combustion) are particularly noteworthy: studies on these seem to have yielded all four of the above-mentioned benefits a–d.

Of the types of catalyst deactivation caused by coking, poisoning, and solid-state transformations, the emphasis in this review is on the last type. Catalyst deactivation by coking and poisoning are quite different types of problems and, as pointed out in section II, these have been covered comprehensively earlier. Deactivation by sintering is also recognized as a separate area. Hence these three causes of catalyst deactivation are practically kept out of the scope of this review. Changes in the chemical composition of the catalyst surface, restructuring or reconstruction of the surface, phase transformations, gradual enrichment/depletion of a particular catalyst component on/from the catalyst surface, these are the topics of prominence in this review. Even here, emphasis is on normally unexpected or unsuspected types of deactivation and the catalyst metamorphosis produced *by the catalytic reaction itself*, as distinct from the purely thermal effects at the reaction temperature; e.g., see the reconstruction of the multicomponent molybdate catalyst during the ammoxidation of propylene to acrylonitrile, given in section III.J.

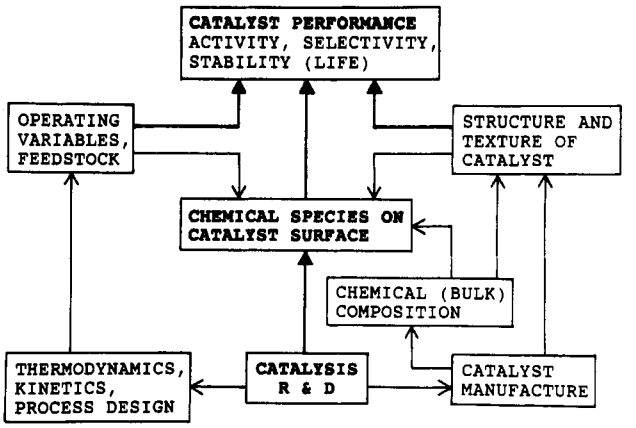

Figure 1. Interaction of various factors which determine the performance of an industrial catalyst (from Menon,[19] copyright 1991 Elsevier).

This review is aimed to provide some essential background information and possibly to serve as a reference guide for trouble-shooting when a catalyst is deactivated for rather mysterious reasons. In this respect, it may be of some use for chemists and chemical engineers engaged in catalysis R&D in both industry and academia and for those engaged in operation of catalytic processes in chemical, petroleum, and petrochemical industries.

II. Catalyst Deactivation in Industry

A. General Aspects

A heterogeneous catalyst is not just a chemical in the ordinary sense of the word. It is a performance chemical or a surface-active material. As is well-known, catalysis occurs only at the surface of such a catalyst. (Here the term "surface" implies the total surface of the catalyst, including that of the micropores, which is accessible to the reactant and product molecules). Hence the performance of the catalyst will depend very much on its surface, which is formed and stabilized under the prevailing process conditions. The nature of the active surface of a "real" catalyst in an industrial process will be determined not only by known and controlled process parameters like temperature, pressure, reactant concentration, and space velocity but also by variable factors like feed composition and unpredictable/unsuspected ones like impurities and poisons in the feed. Figure 1 shows a schematic representation[19] of the interaction of various functions which determine the ultimate performance of a catalyst in an industrial process. In general, the catalyst manufacturer has control only of the chemical or bulk composition and structure and texture of the catalyst, while the catalyst-using industry controls the operating variables and feedstock for the process. All these factors ultimately determine the exact nature of the chemical species and their relative concentrations on the catalyst surface under actual process conditions. Understanding the exact nature of these surface species and fine-tuning them for still better catalyst performance are two of the main tasks of catalysis R&D in industry.

Industries use catalysts in tens or hundreds of tons per year. The cost of a catalyst charge in the plant can

vary from a few thousand to a few million dollars. These catalysts make products worth 100–1000 times their own price. An unexpected and rapid catalyst deactivation, leading to an unscheduled plant shut-down for a change of catalyst, can be an economic disaster. For instance, for a world-scale styrene plant producing about 400 000 metric tons/year of styrene, a change of catalyst will cost a down-time of 7–10 days and a loss of $1 million per day. This is the greatest incentive indeed to investigate how the catalyst was deactivated and how to prevent it in the future.

Catalyst characterization techniques like BET surface area, pore volume, pore-size distribution, metal dispersion, temperature-programmed desorption/reduction/oxidation (TPD/TPR/TPO), X-ray diffraction (XRD), energy dispersive X-ray analysis (EDX), scanning/transmission electron microscopy (SEM/TEM), infrared (IR) spectra are nowadays applied routinely to evaluate and compare catalysts in their fresh state as well as of samples taken from the plant reactor after operation of months or even years. More sophisticated (surface-science) techniques like X-ray photoelectron spectroscopy (XPS or ESCA), Auger electron spectroscopy (AES), secondary-ion mass spectrometry (SIMS), ion scattering spectroscopy (ISS) are also resorted to whenever needed or possible. Such fingerprinting of catalysts has become an essential counterpart to activity/selectivity/life tests in bench-scale reactors, which can closely simulate the actual process conditions in the plant. The importance of such studies has been highlighted in a recent American Chemical Society monograph[20] entitled *Characterization and Catalyst Development: An Interactive Approach.* Since zeolite catalysts have become so important in industrial catalysis in the last few decades, special mention should be made here of the role of XPS in the characterization of zeolite surfaces. Barr and coworkers have used repetitive shifting patterns in the core level[21] and valence band structures[22] for the identification of different zeolite types,[21,23] impurities,[24] degradative byproducts,[24,25] and variations in acidity.[26] The XPS procedures with respect to charging, quantification, and binding-energy referencing have also been described by them in detail.[23,24,27]

A catalyst in a chemical process can undergo deactivation by (a) coke deposition, (b) surface poisoning, and (c) solid-state transformations. A coked catalyst can often be regenerated with only a little loss (2–10% per regeneration) of its original activity. Recovery from effects of poisoning of a catalyst depends upon whether or not it is a case of reversible poisoning, as contrasted to irreversible poisoning and permanent deactivation. Solid-state transformations are generally irreversible under the prevailing process conditions; hence, they lead to irrevocable catalyst damage or destruction. Surface enrichment in catalysts has been reviewed earlier by Menon and Prasada Rao.[7]

The field of catalyst deactivation is of such scientific and industrial importance that international symposia on it are now being held regularly: at Berkeley, CA, in 1978 and 1985, at Antwerp, Belgium, in 1980 and 1987, at Evanston, IL, in 1991, and at Oostende, Belgium, in 1994. The state-of-the-art review lectures and papers presented at these symposia have been published;[28–32] these volumes constitute an important source of literature for catalyst deactivation by coking, poisoning, and solid-state transformations.

1. Coking

Hydrocarbon reactions on solid catalysts at medium or high (above 400 °C) temperatures are invariably accompanied by deposition of carbonaceous materials or "coke" on the catalyst surface, leading to deactivation of the catalyst. Fortunately, most of these cases do not involve any permanent deactivation: the activity can be restored more or less completely by burning off the coke in a carefully controlled manner in a regeneration step. In the case of very rapid coking as in catalytic cracking, the fluidized-bed technique is used for continuous regeneration of the catalyst in very frequent cracking-regeneration cycles. In selective oxidation of hydrocarbons, the coke deposited on the catalyst is continuously gasified by oxygen (air) or steam; this gasification is catalyzed by alkali, which is usually present as a promoter in such catalysts. Excepting for a few cases of broader interest, catalyst deactivation by coking only has been kept out of the scope of this review. State-of-the-art reviews have been given by Froment[33,34] on the kinetics and modeling of catalyst deactivation by coking. Other aspects of coking have also been covered extensively in the earlier symposia on catalyst deactivation.[28–32] It has to be emphasized that coke on catalysts can be of different types, depending on the reactants and products, the nature of the surface (metal, support, acidity, acid-strength distribution, etc.), temperature, partial pressure of hydrocarbons and of hydrogen, etc. Hence the nature and location of coke on the catalyst surface are often more important than the total quantity of coke deposited on the surface. In these and other respects, the coke on the catalyst can be classified as harmful, harmless, invisible, or beneficial, as pointed out by Menon.[35]

2. Poisoning

Starting from the pioneering studies of Maxted in the period from 1920 to 1950 (for a review, see Maxted[36]), catalyst poisoning has now become a fairly mature field. All types of catalysts, metals, oxides, zeolites, homogeneous, heterogeneous, multifunctional, and biological ones, are susceptible to poisons. But the understanding of such phenomena today is much better and the countermeasures to be taken to minimize or prevent them are more generally known than for catalyst deactivation by sintering or other solid-state transformations. Catalyst poisoning has been dealt with comprehensively in two recent monographs by Hegedus and McCabe[37] and Butt and Petersen.[38] Reviews on more specific topics like sulfur poisoning of metal catalysts are available in the books edited by Oudar and Wise[39] and Petersen and Bell.[29] Hence deactivation by catalyst poisoning will not be covered any further in this review except in a few cases where it occurred very surprisingly and in a totally unexpected manner, or along with other modes of catalyst deactivation. It may be emphasized here, however, that prompt diagnosis or a real understanding of catalyst poisoning in industry has become possible in the last 2 decades only due to the availability of, or accessibility to, modern surface-science techniques like EDX, XPS, AES, and SIMS. This aspect will be stressed in some of the case histories cited later in this review.

3. Sintering/Redispersion

Traditional mechanisms of sintering of supported-metal catalysts consist of migration and coalescence of the crystallites or particles and global or local ripening (for a review, see Ruckenstein and Sushumna[40]). Ruckenstein[41] has recently proposed that mechanisms involving wetting and spreading can also be relevant. In an oxygen atmosphere, both the small and large metal crystallites emit patches (visible under electron microscope) of multilayer films. These patches can coalesce to generate a continuous film among a large number of crystallites. In a hydrogen atmosphere, the films are reduced and they rupture, generating patches surrounding the already existing metal particles or independent patches which contract generating totally new particles. Thermodynamic considerations are employed to explain film formation in an oxygen atmosphere and film rupture in a hydrogen atmosphere. Both these phenomena are driven by the general tendency of decrease of the free energy of the system. In this context, the evolution of different particle shapes in different gas environments is also important; this can even by used to control particle shape in supported metal catalysts, as demonstrated for Pt particles by Lee et al.[42]

B. Some Causes for Surface Enrichment/Depletion

Elementary thermodynamic considerations can show that the creation of a surface is accompanied by a positive free energy change. In order to minimize this positive free-energy change, the constituent which has the lowest free energy tends to migrate to the surface. Thus the differences in the surface free energies of the components in the solid system lead to the surface enrichment of the topmost layer with constituents having the lowest surface energies. Several thermodynamic models have been developed to predict the surface composition of ideal or regular solid solutions; Overbury et al.[2] and Somorjai[6] have reviewed these models in detail and also presented some typical calculations of the model systems for surface enrichment.

Since the migration of a constituent of a solid from its interior to its surface usually involves an activation energy barrier to be overcome, such a process necessarily requires a higher temperature. As a rule of thumb, the Tammann temperature (ca. half the melting temperature in kelvin) is generally believed to be sufficient to make the atoms or ions in the bulk to be mobile enough for such bulk-to-surface migrations, while the Hüttig temperature (ca. one-third the melting temperature in kelvin) is enough to make the species, which are already on the surface, adequately mobile to undergo agglomeration or sintering. Table 1 gives the Hütting temperatures for the metals that are most commonly used as catalysts. These temperatures are quite low, often below the process temperature at which such metals are used as catalysts. How can these metals then ever be used as practical catalysts? Therein lies the art of catalyst making: these metals are never used alone as catalysts; they are invariably deposited or supported on suitable carriers which anchor the tiny metal crystallites and prevent their free motion or migration under typical process conditions.

Table 1. The Hüttig Temperature of Some Common Catalytic Metals, Calculated as One-Third of the Melting Point

Metal	Ag	Cu	Ni	Fe	Pd	Pt
Hüttig temp, °C	138	179	302	330	335	403

Even if the nominal temperature at which a catalytic reaction is carried out is below the Hüttig temperature for the components in the solid catalyst, the actual temperature on the catalyst *surface* can be much higher in the case of exothermic reactions. The situation becomes still worse since many oxides (used as the catalytically active species and/or as supports) are very poor conductors of heat; hence, the heat of the exothermal reaction cannot be dissipated rapidly. This can lead to the formation of "hot spots" on the catalyst particles. In the case of partial oxidation of hydrocarbons, an increase in temperature leads to the thermodynamically more favored complete combustion of the hydrocarbons into CO_2 and water. Since the heat of combustion of a hydrocarbon is about 8–10 times higher than that of its partial oxidation, this can lead to run-away temperatures and explosive situations. For commercial operation of such processes, fluidized-bed reactors or shell-and-tube heat-exchanger-type reactors are commonly used. In spite of such elegant practical engineering solutions to the acute heat-transfer problem, the local overheating on catalyst surfaces can sometimes result in run-away temperatures, melting of the catalyst tubes in the reactor, or bulging of high-pressure reactor walls. The surface enrichment or depletion of the catalyst during these high-temperature excursions often leads to a significant loss of catalytic activity and selectivity. This forces the plant into a costly shut-down for several days to cool down the reactor, discharge the deactivated catalyst from the reactor, take in a fresh charge, and bring it up to operating temperature.

Another cause for gradual surface enrichment or depletion is the tendency of some catalyst components to form volatile compounds with one of the reactant species. Thus nickel can be slowly stripped off a catalyst surface as volatile and thermally unstable nickel carbonyl if the reaction mixture contains CO, even as an impurity. The volatilization of molybdenum oxide in the presence of steam from molybdate catalysts in industrial processes is well-known. For instance, in the ammoxidation of propylene to acrylonitrile on multicomponent molybdate catalysts, the sublimation of MoO_3 from the catalyst and its condensation on the cooling coils in the fluidized-bed reactor upsets the normal temperature control of the reactor; sometimes the plant has to be shut down only to scrape off the molybdena scales from the cooling coils and restore the heat-transfer efficiency of these coils. Substantial loss of Ru by volatilization as ruthenium oxide occurs when supported Ru catalysts are used at high temperatures; one way to minimize this is to add as promoters oxides of Ca, Sr, or Ba, which can bind Ru as the corresponding ruthanate in its oxidized form and thus prevent volatilization of its oxide. Such phenomena may also be expected if volatile organometallic compounds can be formed between any of the reactants or products in a process and a metallic species in the multicomponent catalyst used, but these do not seem to have been much

suspected or investigated as a cause for catalyst deactivation so far.

Chemisorption-induced surface enrichment of a multicomponent surface may occur due to the differences in the heats of adsorption of the gas or vapor on the different components. The species forming the stronger chemisorption bond with the adsorbate tends to be pulled up from the inner atomic layers and to accumulate on the surface.

C. Monolayer Dispersion of Oxides on Substrates

One of the important steps in the preparation of supported metal or oxide catalysts is the calcination after the impregnation of the salt(s) on the catalyst carrier or support. For supported metal catalysts, e.g., alumina-supported Pt or Pt–Re and such bimetallic catalysts for catalytic reforming of naphtha to high-octane gasoline or to aromatic feedstocks for the petrochemical industry, it is well-known at least for the last 30 years that the catalyst should be calcined at 500 °C for a few hours before the reduction step. Only then, a high dispersion of Pt will be obtained on the alumina. The exact reason for this calcination has been attributed to the necessary decomposition of the metal salt to its oxide form and the removal of water, which can otherwise sinter the freshly reduced metal. An equally important factor, perhaps less recognized till recently or even now, is the spontaneous monolayer dispersion of oxides and salts on to surfaces of support substrates. This is particularly important in the preparation of mixed-oxide catalysts. Considerations of equilibrium conditions at the interface between two solid phases and the gas phase can explain the transformations which are possible. For instance, when the energy of cohesion of the clusters of a supported oxide is smaller than the energy of adhesion of this oxide to the underlying support, spontaneous spreading of the former over the surface of the latter will take place. This is the phenomenon of wetting. As the energy of wetting of V_2O_5 is smaller than its energy of adhesion to anatase or alumina, V_2O_5 can wet these supports and spread over their surface. Conversely, when V^{5+}–O clusters are reduced to V^{3+}–O clusters, the energy of cohesion increases to such an extent that it becomes greater than that of its adhesion to the support; the monolayer of vanadium oxide then shrinks and coalesces into three-dimensional particles or islands on the support surface. Exposure of a supported vanadia catalyst to an oxidation–reduction cycle can thus lead to a complete restructuring of the surface. Haber[43] has reviewed these and several other basic aspects of oxidation catalysts in 1992. Xie and Tang[44] gave an excellent review on "Monolayer Dispersion of Oxides and Salts onto Surfaces of Supports: Applications to Heterogeneous Catalysis" in 1990. Some typical examples of monolayer dispersion are given in Table 2. If this dispersion step is inadequate or incomplete, the resulting oxide layer, and any reduced-metal surface from it, will not be reproducible: from the same catalyst system, one can then have different catalysts prepared at different times, and of course from one laboratory to another.

Haber[43] emphasizes that oxide surfaces are in dynamic interactions with a reacting gas phase. The oxide phase may respond to the change of composition of the reacting catalytic mixture in three ways: (1) defect equilibria at the oxide surface or in the bulk may be shifted and the concentration of a given type of active site can change, causing a change in catalytic properties; (2) when the concentration of defects at the oxide surface exceeds a certain critical value, ordering of defects or formation of a new two-dimensional surface phase may occur, resulting in a dramatic change of catalytic properties; (3) in case of redox reactions of the catalyst, as in the well-known Mars–van Krevelen type mechanisms for hydrocarbon oxidation, the ratio of the rates of reduction and reoxidation may be different for the various oxide phases in the catalyst; this can lead to time effects or hysteresis in the dependence of catalytic properties on the composition of the gas phase and hence strong lingering or slowly-decaying effects of catalyst pretreatment.

Table 2. Some Typical Examples of Systems Displaying Spontaneous Monolayer Dispersion (Adapted from Xie and Tang[44])

			heat treatments	
support	compound	mp (°C)	°C	h
γ-Al_2O_3	MoO_3	795	350–450	24
	$CuCl_2$	498	350	24
	CuCl	422	350	2
	V_2O_5	690	650	34
	$FeCl_3 \cdot 6H_2O$	37	70	78
	$Fe(NO_3)_2 \cdot 9H_2O$	47	30	89
	$NiNO_3 \cdot 6H_2O$	57	30	89
SiO_2 gel	MoO_3	795	450	14
active C	$HgCl_2$	276	25	24
	$ZnAc_2$	242	105	22
TiO_2	MoO_3	795	400	24

D. Rate-of-Heating Effects

In the preparation steps for a catalyst like precipitation, calcination, and reduction, heating rates could sometimes be very important. Since 1978, it is known that too high temperatures during reduction of titania-supported metal catalysts can lead to the so-called strong metal-support interaction or SMSI. This can be caused by migration of the partly reduced TiO_x species on to the metal surface, the so-called "decoration" effect (for a review of SMSI, see Burch[45]). The rate-of-heating effect (ROHE) is not so commonly appreciated in catalysis. One exception may be ZSM 5-type species, for which it is generally known that the template has to be decomposed off at a *slow* heating rate in a stream of oxygen.

ROHE can be more spectacular in the case of reduction of metallic catalysts. For instance, Ertl and co-workers at Berlin showed that a slow reduction/activation of ammonia synthesis catalyst can lead to small highly crystalline α-iron platelet structures (as seen in scanning electron micrographs), with a BET surface area of 18 m^2/g and a relative catalytic activity of 1 for ammonia synthesis; when a shock reduction was carried out, the SEM showed typical pine-apple-tree structures (demonstrating segregation of separate promoter phases), with a BET surface area of 15 m^2/g and a relative catalytic activity of only 0.5 (cf. Mahdi et al.[46]). Still more detailed pictures of the catalyst (or of the species in it or on it) are obtained from *in situ* X-ray absorption fine structure (EXAFS) and X-ray

absorption near edge structure (XANES) techniques, as shown quite recently by Rao and co-workers[47] at Bangalore, India. When Cu/ZnO and Cu/ZnO–Al_2O_3 methanol synthesis catalysts are reduced, they contain Cu microclusters, species of Cu^{1+} dissolved in ZnO, metallic Cu, and Cu_2O. The proportions of these different phases critically depend on the *heating rate* during reduction. A faster heating rate of 10 K/min predominantly yields the metal species (>50%), while a slower rate of 0.8 K/min enhances the proportion of the Cu^{1+} species (to about 60%). Reduced Cu/ZnO–Al_2O_3 shows the presence of metallic Cu (up to 20%), mostly in the form of microclusters and Cu^{1+} in ZnO as the major phase (about 60%). The addition of alumina to the Cu/ZnO catalyst seems to favor the formation of Cu^{1+}/ZnO species. According to Duprez et al.,[48] these are the species associated with the catalytic activity for methanol synthesis. If the relative concentration of the really active catalytic species can be increased just by a slower rate of heating during reduction, surely ROHE deserves far more attention than has been the case so far.

E. Need for Time-Resolved Catalyst Characterization

Most of the catalyst characterization studies so far are for the state of the catalyst at a particular instant, either before the catalytic reaction or after the reaction. In this respect, they are just "snapshots" of the catalyst. For a better understanding of the catalytic phenomenon, however, more and more *in situ* measurements are necessary. Also, there is an increasing need to follow the changes of the catalyst as a function of time. Experimental techniques like hot-stage electron microscopy, NMR, IR spectroscopy, Mössbauer spectroscopy, XRD, and EXAFS are suited to follow the changes in/on the catalyst in an *in situ* time-resolved manner. Such measurements are just being reported in the literature.[49–53]

III. Case Histories

Several case histories are cited below to illustrate how a detailed characterization of equilibrium/spent/deactivated catalysts led to a better understanding of (a) the "real" surface of the catalyst under actual process conditions and (b) the true causes of catalyst deactivation; this led to effective countermeasures being taken to minimize or prevent such deactivation from occurring again. Only one or two typical examples each for various major catalytic processes will be given; no attempt will be made here to collect all the relevant cases for any one process, since such information is readily available in reviews devoted to that particular process.

A. Iron Catalyst for Ammonia Synthesis[54,55]

This is a classic catalyst. Research work on it worldwide has continued for the last 80 years. It was during the course of these studies that some of the landmarks in catalysis were developed for the first time, e.g., the Brunauer–Emmett–Teller (BET) method for determination of total surface areas of porous adsorbents and catalysts and specific chemisorption techniques for metal dispersion in multicomponent or supported metal catalysts. Using these adsorption

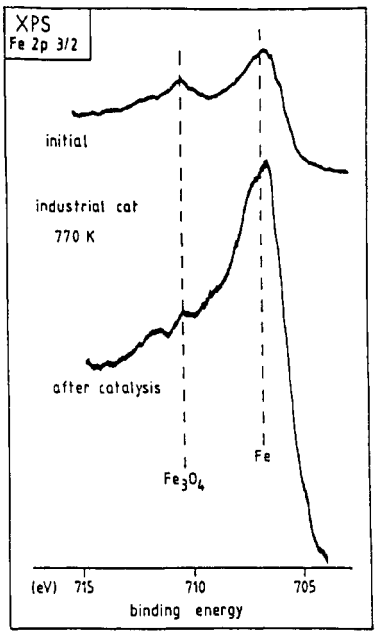

Figure 2. XPS data of a sample of doubly promoted iron catalyst immediately after reduction and after use in ammonia synthesis at atmospheric pressure (from Mahdi et al.,[46] copyright 1991 J. C. Baltzer AG, Basel).

techniques, Emmett and Brunauer[56] showed that (a) the small amounts of promoters potassium and alumina cover a significant part of the catalyst surface, (b) in small amounts free alumina is not present on the surface, whereas in larger amounts it ends up as a separate phase on the surface, and (c) in the absence of alumina, potassium will be lost from the catalyst under ammonia synthesis process conditions; thus one role of alumina is to stabilize the iron surface structurally and to prevent the loss of potassium promoter. These conclusions of Emmett and Brunauer were confirmed about 40 years later by Silverman and Boudart,[57] who used not only the chemisorption techniques but also modern characterization techniques like Auger electron spectroscopy and Mössbauer spectroscopy. Using low-energy ion scattering spectroscopy (LEIS), Davis[58] has also demonstrated that the surface of a typical fused iron commercial ammonia synthesis catalyst is largely covered by promoter oxides of Ca and/or K; complementary photoemission results indicate that atomic nitrogen is deposited in the near-surface region during catalyst activation in NH_3/H_2 mixtures.

Ertl and co-workers at Berlin and Somorjai and co-workers at Berkely used surface-science techniques like XPS, UPS, and ISS to characterize ammonia-synthesis catalysts (both commercial catalysts and model single-crystal planes of iron). Their studies have been summarized in three chapters in the book *Catalytic Ammonia Synthesis—Fundamentals and Practice*, edited by Jennings.[55] Typical Fe signals in the X-ray photoelectron spectra of a doubly-promoted commercial ammonia-synthesis catalyst after its reduction and after its use in ammonia synthesis at atmospheric pressure, taken from the work of Mahdi et al.,[46] are shown in Figure 2. The reduction of Fe^{3+} oxide surface to a Fe^0 metallic surface continues during ammonia synthesis for about 100 h. The elemental composition of the activated catalyst surface, determined by XPS, was (in atomic %) Fe, 48; O, 31; Al, 8; K, 5; Ca, 2; and C (impurity), 6. This composition and the strong domi-

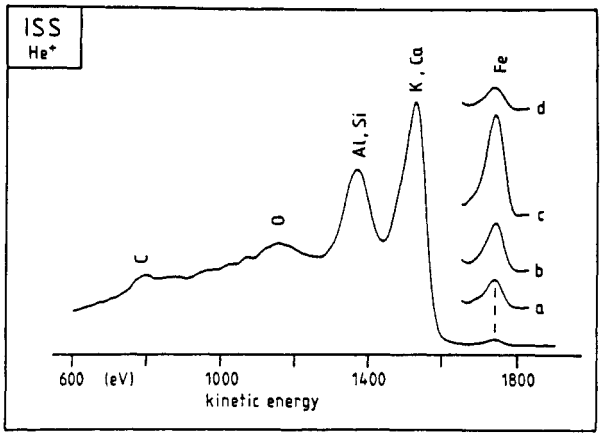

Figure 3. He-ion scattering spectra of doubly promoted ammonia synthesis catalyst surface, showing the assignment of elements in the top surface layer. The inset (a, b, c, and d) is the Fe signal shown for various treatments (see the text) on the same intensity scale (from Mahdi et al.,[46] copyright 1991 J. C. Baltzer AG, Basel).

nance of the zero-valent iron (Figure 2) led to the conclusion that the surface consists of islands of iron metal between areas of promoter deposits. A significant amount of contaminant water accounts for the excess oxygen over the metal ions. This water does not react with the iron metal, presumably because a thin layer of promoter material prevents the intimate contact of the water with the iron surface.

The depth of penetration of XPS measurements is a few (three to eight) atomic layers from the surface. A truly surface-sensitive technique is ion scattering spectroscopy (ISS), which can scan the top-most layer only and give results just as from specific chemisorption measurements. The He-ion scattering spectra of ammonia-synthesis catalyst (same sample and same conditions as for the XPS data in Figure 2), also reported by Mehdi et al.,[46] are shown in Figure 3. The reduced catalyst shows on its surface the signals of C, O, Al, Si, K, Ca, and only a small signal of Fe. Only about 10% of the exposed surface consists of iron atoms. Uncertainties in quantitative ISS calibration make it difficult to give an exact surface composition, but the sensitivity of the technique is shown by the changes of the Fe signal (inset) of the free iron surface when the conditions/atmospheres are changed: (a) at 300 K in UHV; (b) at 760 K in UHV, due to desorption of gases more Fe surface becomes free; (c) when H_2 is introduced at 10^{-5} mbar and 760 K, some chemisorbed N species on the iron surface are reacted off as ammonia, exposing still more free Fe; (d) when a mixture of $3H_2$–N_2 is introduced at 10^{-5} mbar, once again NH_x species are formed and they cover a good part of the free Fe sites on the surface. The presence of chemisorbed nitrogen on the surface, unfortunately, cannot be observed directly in ISS due to the very low cross section for N. From the apparent discrepancy between ISS and XPS data, Mahdi et al. suggest that the promoter atoms are mainly present as a very thin film transparent for XPS, but shielding the contamination layer of water from the iron metal. These studies serve as a typical example to illustrate how a combination of modern surface characterization techniques can give a fairly detailed picture of practical catalyst surfaces and the changes occurring there almost at the atomic or monolayer scale.

The ammonia synthesis catalyst and process have been perfected to such an extent that present-day catalysts have normally a life of 5–10 years. However, operational mishaps do occur sometimes, necessitating a change of catalyst charge. Poisoning of the iron catalyst can be caused by oxygenated compounds like CO, CO_2, and H_2O, but this is mostly reversible provided the poison levels are low and the exposure is not for long periods of several days. Irreversible poisoning is caused by traces of S, Cl, As, P, etc. Deactivation by thermal sintering of the iron catalyst is fortunately a very slow process, the original surface area of about 15 m^2/g decreasing to 10 m^2/g in about 5 years. In older ammonia plants, ammoniacal copper liquor was used for removal of CO; process upsets could then sometimes carry over some copper to poison the iron catalyst. This is no longer a problem in modern plants, where the CO removal is achieved by a low-temperature CO-shift reaction and complete methanation of any residual CO still left over. Still another cause for deactivation of the catalyst could be a physical covering of the iron surface by inert material; e.g., amorphous carbon is deposited by thermal or catalytic cracking of higher hydrocarbons from compressor lubricating oil. Small levels of carbon are removed from the surface as methane; still permanent damage can occur to the catalyst just because small leaks of compressor oil are so hard to detect. Another stipulation is on the use of only sulfur-free lubricants. Modern centrifugal compressors and circulators normally meet all these stringent specifications and they do not introduce any significant amounts of oil into the gas-circulation loop in the plant. However, slugs of oil can still be introduced inadvertently during process interruptions or operational upsets.

An extremely subtle deactivation of the ammonia synthesis catalyst can occur[59] during its very first reduction in the plant reactor. The reduction has to be carried out with a very high space velocity of the reducing gas to sweep away the water formed in the reduction, otherwise this water will favor sintering of the freshly reduced iron catalyst in the lower layers of the catalyst bed. In spite of taking this precaution, the BET surface area of the reduced catalyst can be appreciably different from the top to the bottom of the bed, as shown in Figure 4. The only way to overcome this problem is prereduction in a very controlled way and in much smaller catalyst layers, followed by a passivation of the (otherwise pyrophoric) catalyst by the catalyst manufacturer before the catalyst is sent to the user plant. In the plant, a quick and relatively mild reduction is enough to remove the skin-oxide layer formed during passivation. Most catalyst manufacturers offer now both unreduced and prereduced + passivated ammonia-synthesis catalysts.

The problems of catalyst deactivation by poisoning and other causes are important not only in ammonia synthesis but also in its upstream processes like water–gas generation, CO-shift conversion, and purification of synthesis gas in various steps. These have been dealt with in detail in *Catalyst Handbook*, edited by Twigg.[44] This is an excellent reference source for a good deal of practical information on industrial catalysts, on their uses, and on handling them safely; such information is rarely seen in other publications in the area of catalysis.

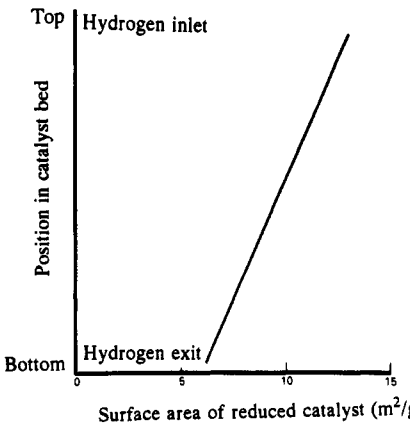

Figure 4. Variation in total surface area of ammonia-synthesis catalyst as a function of its position in the catalyst bed during reduction. Water, produced by the reduction of catalyst in the upper part of the bed, causes the sintering of the catalyst in the lower layers (from Spencer,[59] copyright 1989 M. V. Twigg).

The comprehensive treatise, edited by Jennings,[55] *Catalytic Ammonia Synthesis—Fundamentals and Practice* was also published in 1991.

B. Support Methanation in Ru-Catalyzed Ammonia Synthesis

In 1991, British Petroleum and Kellogg jointly announced the development of a new process for ammonia synthesis, using ruthenium supported on a high-surface-area graphite carrier as the catalyst. One of the most difficult problems encountered during the development of this catalyst was the methanation of the graphite support itself. This can undermine the long-term performance of the catalyst due to mechanical disintegration of the support structure. Ultimately a methanation-resistant graphite support had to be developed (Knez et al.[60]).

C. Methanol Synthesis

The catalytic synthesis of methanol is considered a well-proven technology on a large scale. That is why methanol was recognized as the intermediate to start with for the synthesis of other chemicals in the new C_1-chemistry, developed in the wake of the energy crisis (Chang[61]). Significant achievements in the fuel area are the Mobil methanol-to-gasoline (MTG) process and the large-scale production of the octane-booster additive methyl *tert*-butyl ether (MTBE) from methanol and isobutene (cf. Wender[62]).

Present-day low-pressure methanol-synthesis catalyst consists of CuO and ZnO on an alumina support. The conventional poisoning and deactivation by various causes of this catalyst have been discussed in detail, e.g., by Bridger and Spencer.[63] For the purposes of this review, it is more relevant and important to point out that catalyst deactivation could also occur by several other extraneous and often totally unsuspected contaminants. A list of these for methanol synthesis is given in Table 3. Some of these contaminants are of equal importance in the manufacture and use of a whole range of other industrial catalysts also, though the effects of these on the process concerned could be quite different from those shown in Table 3 for methanol synthesis.

In recent years, liquid-phase or slurry processes for methanol synthesis have received considerable attention.[64,65] From these developments, just one example is cited here to show how the problem of acute catalyst deactivation can sometimes be circumvented by clever process adaptation: two severe catalyst poisons of a separate two-step catalytic process are rendered harmless when the two steps are telescoped into a double-catalyst single-reactor process, as described below.

The advantages of a liquid-phase process for methanol synthesis are at least two-fold: (a) thermodynamically methanol synthesis is favored at lower temperatures and (b) heat dissipation in the liquid phase is easier than in the gas phase for an exothermic process like this. The two reactions involved in the liquid-phase are the carbonylation of methanol to methyl formate at 60–90 °C and 30–65 bar pressure, homogeneously catalyzed by alkali alkoxide, e.g., potassium methoxide, and the hydrogenolysis of the methyl formate to two molecules of methanol on a copper chromite catalyst in a slurry reactor at 140–180 °C and up to 75 bar pressure. The net reaction is of course the combination of two molecules of H_2 with one molecule of CO to yield methanol:

$$CH_3OH + CO \rightarrow HCOOCH_3$$
$$HCOOCH_3 + 2H_2 \rightarrow 2CH_3OH$$
$$2H_2 + CO \rightarrow CH_3OH$$

Onsager,[66] Onsager et al.,[67] and Liu et al.[68] have reported the synthesis of methanol in a single reactor, combining the carbonylation and hydrogenolysis reactions, using as catalyst a combination of sodium or potassium methoxide and copper chromite. This is known as the concurrent synthesis of methanol. In the two-step process, water and CO_2 are poisons for the

Table 3. Effects of Possible (but Often Unexpected or Unsuspected) Contaminants and Poisons on $Cu/ZnO/Al_2O_3$ Catalysts for Methanol Synthesis (from Bridger and Spencer,[63] Copyright 1991 M. V. Twigg)

contaminant/poison	possible source[a]	effects
silica, other acidic oxides	transport in steam in plant gases	waxes, other byproducts formed
γ-alumina	catalyst making	dimethyl ether formed
alkali	catalyst making	decreased activity, higher alcohols formed
iron	transport in plant as $Fe(CO)_5$	methane, paraffins, waxes formed
nickel	transport in plant as $Ni(CO)_4$	methane formed; decreased activity
cobalt	catalyst making	methane formed; decreased activity
lead, heavy metals	catalyst making	decreased activity
chlorine compounds	transport in plant gases	permanent decrease in activity
sulfur compounds	transport in plant gases	permanent decrease in activity

[a] Raw materials for catalyst manufacture, if not of sufficient purity, can also be a source of contamination.

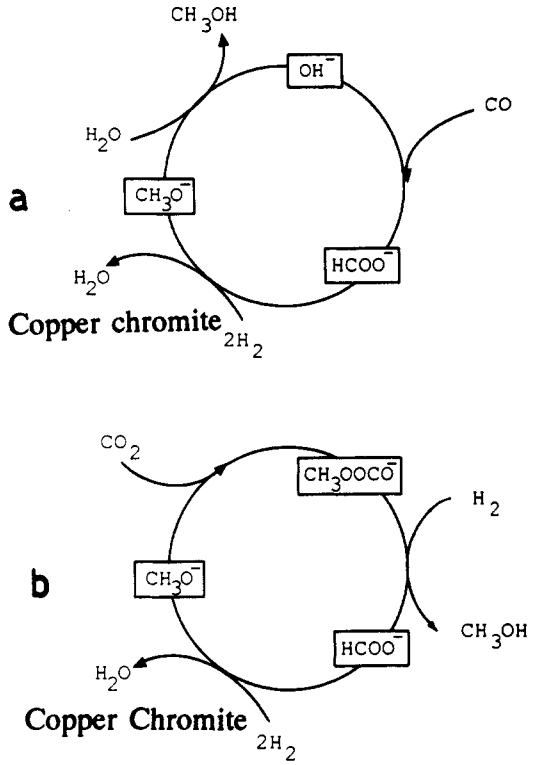

Figure 5. Both H_2O and CO_2 are normally poisons for the potassium methoxide catalyst. In the presence of copper chromite catalyst, they are reacted away (a, for H_2O; b, for CO_2) and thus rendered harmless while the methoxide catalyst (CH_3O^-) is regenerated to continue the catalytic cycle (from Palekar et al.,[69] copyright 1993 Elsevier).

alkoxide catalyst, since they react with the alkoxide to form alkali formate (HCOOK) and alkali methyl carbonate (CH_3OOCOK), respectively. The concurrent process, on the other hand, is superior in this respect and also exhibits some remarkable synergism (Palekar et al.[69]): (a) the overall reaction rate is higher than predicted for either the carbonylation or the hydrogenolysis reaction, (b) the copper chromite regenerates the potassium methoxide catalyst for carbonylation when it is poisoned by traces of water or CO_2, (c) the chromite catalyst also reacts away any trace of water by the water–gas shift reaction ($CO + H_2O \rightarrow CO_2 + H_2$), and (d) the carbonylation reaction takes place in the pores of copper chromite and thus supplies additional reactant *in situ* for the hydrogenolysis reaction. Figure 5 shows the reaction networks, proposed by Palekar et al.,[69] for the elimination of H_2O and CO_2, which are poisons for the potassium methoxide catalyst; both the networks end up in the formation of methanol and the regeneration of the methoxide catalyst.

D. Catalytic Reforming

This is the process to convert naphtha or other petroleum fractions with low research/motor octane number (RON/MON) to gasoline fractions with higher octane number or naphtha to aromatic feedstocks for the petrochemical industry. Reforming is mostly re-forming the molecular shape without changing much the carbon number of the molecules: converting six-membered naphthenes to aromatics by dehydrogenation, five-membered naphthenes to aromatics by ring expansion and dehydrogenation, straight-chain paraffins to branched ones by isomerization or to aromatics

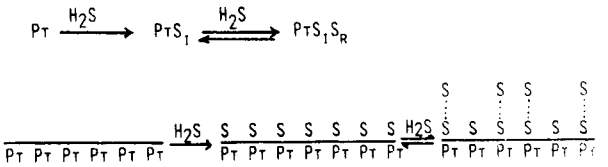

Figure 6. Schematic representation of reversibly held sulfur over an irreversibly held layer on the entire Pt metal surface under reforming conditions (adapted from Menon and Prasad[71]).

by dehydrocyclization, etc. Carbon–carbon bond fission as in dealkylation, cracking, or hydrocracking also occurs to a limited extent. The reforming process is usually carried out on a bifunctional catalyst in three or four catalyst beds at 490–510 °C and a hydrogen pressure of 10–20 bar.

Haensel and Haensel[70] recall a case from the early history of catalytic reforming on the first-generation monometallic Pt/alumina catalyst. In early 1950s when several reforming plants were running smoothly, one particular plant exhibited a rapid catalyst deactivation. At that time, microanalysis was still in its infancy and gas chromatography had not even been discovered yet. A careful analysis of the deactivated catalyst from the top of the bed showed traces of arsenic. To find arsenic in the feedstock, large volumes of the naphtha had to be extracted with sulfuric acid and the extract concentrated until a positive analysis for As was obtained. Indeed, the naphtha contained As: 35 parts per *billion* (ppb)! Once the cause of catalyst deactivation was clearly established, the remedy was at hand. A guard bed of clay balls removed all As from the naphtha and protected the reforming catalyst to give a normal cycle life.

With the advent of the bimetallic Pt–Re–alumina catalysts, the role of sulfur in catalytic reforming became puzzling. The feedstock naphtha always contains some sulfur compounds; this sulfur will be converted to H_2S under reforming process conditions. The bimetallic catalyst cannot tolerate more than 1 ppm S, while the monometallic Pt–alumina could work with up to 20 ppm S in the naphtha. The reason for this disparity was studied by Menon and Prasad.[71] Their results showed that under reforming conditions all surface Pt atoms were sulfided irreversibly (S_i), over which a reversibly adsorbed layer of sulfur (S_r) could also build up (Figure 6), depending upon the partial pressure of H_2S (which, in turn, is proportional to the sulfur content of the naphtha):

$$Pt + H_2S \rightarrow PtS_i$$

$$PtS_i + H_2S \rightleftarrows PtS_iS_r$$

For Pt–alumina, some reversible sulfiding is necessary over and above the irreversibly sulfided layer to suppress hydrogenolysis and enhance aromatization. For Pt–Re–alumina, irreversible sulfiding already achieves these; hence, any further S will only decrease the overall activity. Hence the S tolerance of the bimetallic catalyst is <1 ppm, whereas for the monometallic catalyst it can be up to 20 ppm. Once the reasons for these sulfur tolerances are known, the desulfurization specifications for the naphtha can be fixed accordingly. Several subsequent investigations during the last 15 years have confirmed the above concepts of irreversibly and

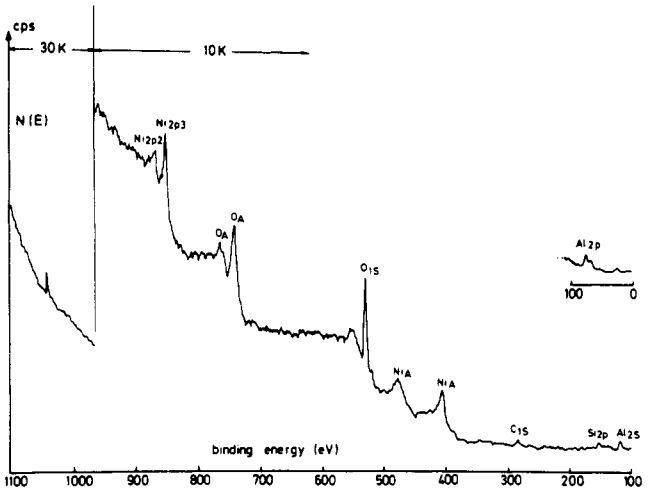

Figure 7. X-ray photoelectron spectrum of a Ni/α-alumina catalyst, deactivated in steam reforming of methane (from De Deken et al.,[75] copyright 1981 Academic Press).

reversibly adsorbed sulfur on the metals and their distinct roles in catalytic reforming.[72] For a recent review, see Bickle et al.[73] and the Chapter by Parera and Figoli in ref 16.

E. Steam Reforming

Steam reforming is the most important process today to convert hydrocarbon feedstocks like naphtha, LPG, or natural gas into synthesis gas for its further conversion to hydrogen, ammonia, ammonia-based fertilizers, nitric acid and other products, and methanol. It is carried out at 700–900 °C on a supported nickel catalyst in the presence of superheated steam. For a general review, see Rostrup-Nielsen.[74]

During the conventional operation of the steam-reforming process, it is necessary to add some (recycle) hydrogen into the reaction mixture to keep the nickel in the catalyst in its proper reduced form (or to prevent its reoxidation by steam). If this hydrogen recycle is cut off, the catalyst undergoes an irreversible deactivation. De Deken et al.[75] made a comparative study of the active catalyst (operated with H_2 in the feed) and the deliberately deactivated catalyst (by cutting off H_2 from the feed) in steam reforming of methane. The techniques employed were the temperature-programmed combustion (TPC) of "coke" on the catalyst samples and XPS. The carbon in the active catalyst burns off mostly before 500 °C. The carbon in the deactivated catalyst shows maximum combustion at about 50 °C higher temperature than that of the active catalyst; the combustion also continues at higher temperatures and is complete only after 150 min at 720 °C. From the cumulative amount of CO_2 evolved, the C content of the active and deactivated catalysts amounted to 0.023 and 0.039 wt %, respectively. From the evolution of 30% of CO_2 only above 600 °C, this part of the carbon seemed to be *not on the surface* but in the bulk of the Ni crystallites. This inference was checked and confirmed by XPS. The overall XPS scan (Figure 7) of the deactivated catalyst shows the peaks of Ni, Al, O, and C. Peak analysis indicates that Al is present as Al_2O_3 (Al_{2p} binding energy, BE, of 74.7 eV), while O has an oxide band (531.6 eV) for Al_2O_3. Ni is identified as NiO ($Ni_{2p3/2}$, 852.3 eV). The C peak shows a shoulder formation on the lower energy side. This peak can be

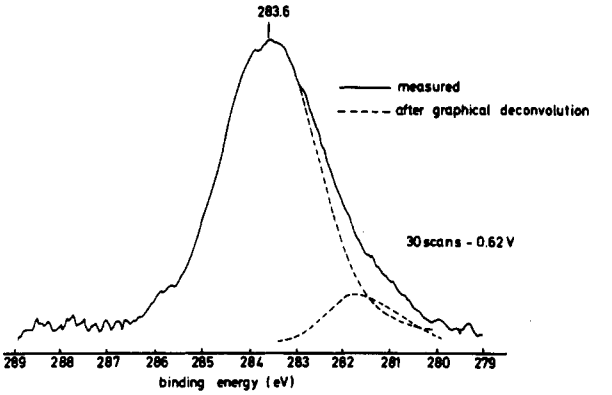

Figure 8. Deconvolution of the signal averaged C_{1s} peak in the X-ray photoelectron spectrum of the deactivated steam reforming catalyst (from De Deken et al.,[75] copyright 1981 Academic Press).

Table 4. XPS Analysis of Elemental Composition of a Deactivated Steam-Reforming Catalyst after Ion Sputtering to Different Depths[a] (from De Deken et al.,[75] Copyright 1981 Academic Press)

sputter time (min)	0	3	10	20	30
ca. etching depth (nm)	0	5	17	34	68
element (at %)					
Ni	6.3	9.5	10.1	12.3	11.1
Al	25.7	25.1	31.3	28.5	31.6
O	54.4	52.5	47.9	52.8	54.3
C	13.6	12.8	10.7	6.4	3.0

[a] Note the continuous decrease of C content with increasing penetration from the surface, while the Ni content increases up to about 5 nm and thereafter remains practically constant. Due to shake-out and shake-up phenomena and differences in escape depth, the relative error in atomic concentrations determined by XPS could be 10–15%. To improve upon this, the authors have adopted the more accurate method of C. D. Wagner (*Anal. Chem.* **1972**, *44*, 1050).

deconvoluted (Figure 8) into the major C_{1s} "graphite" (amorphous or crystalline, no distinction possible here with XPS) peak with a BE of 283.5 eV and a C component where C_{1s} has a BE of 281.7 eV. The energy shift of 1.7 eV for the latter peak is of the same order as seen for C in carbides of metals like Ta, Ti, V, W, and Zr. Hence, it could be due to the presence of Ni_3C in the surface and subsurface layers of Ni. By ion sputtering, layer after layer from the catalyst surface was removed and from periodic XPS analysis a depth composition profile could be determined (Table 4). After ion sputtering, Ni was detected as metallic Ni (no longer as NiO, as on the surface), whereas no change occurred for the Al and O peaks. The C peak decreased continuously with sputter time upto a depth of over 60 nm from the surface. The XPS study thus confirms the indication from the TPC of coke that, in the deactivated catalyst, C has diffused or dissolved into the bulk of Ni. Furthermore, a part of this C is in the carbidic form (perhaps formed on cooling the catalyst from 700 °C, since Ni_3C is thermodynamically unstable above 400 °C).

Hoste et al.[76] have reported an interesting case history of the rapid deactivation of a Ni/α-Al_2O_3 commercial catalyst during methane-steam reforming studies in a laboratory bench-scale unit. In plant practice, this catalyst gives fairly stable performance for periods of 10–20 months or more, but in the laboratory unit it was deactivated in 6–8 h. XPS studies showed an accumulation of Si and Pb on the deactivated catalyst

from the laboratory unit. A closer examination of this unit part by part suggested that Si might have had its origin in the alundum balls used as a support and in the preheating zone for the catalyst bed (Si is volatile in steam to some extent). The source of Pb was traced back to the steam generator of the unit. Distilled water flowing through a metallic valve at 20 °C was leaching out the Pb present as a construction material of the valve and depositing it on the catalyst. When a Teflon valve was used instead of the metallic valve, this peculiar laboratory poisoning of the industrial Ni catalyst by Pb was eliminated.

F. Selective Hydrogenation

Boitiaux et al.[77] have surveyed the general problem of poisoning of various catalysts used for selective hydrogenation of unsaturated hydrocarbons in petroleum refining and in petrochemistry. Usually this is a partial hydrogenation of acetylenic triple bonds to the corresponding olefinic double bonds or of multiple double bonds into the corresponding mono-olefin, but not further to the paraffinic stage. Such selective hydrogenations are commonplace in the downstream processing of intermediate products from steam cracking, fluid catalytic cracking, and coking/visbreaking processes. Boitiaux et al.[77] emphasize that catalyst-deactivation problems arising in this area can be understood properly only if the three components, the catalyst, the impurity, and the hydrocarbons, are all considered in a triangular matrix at the operating conditions of the process, particularly the temperature. The effect of one catalyst poison may be accentuated or attenuated by a second poison. For instance, the poisoning effect of sulfur on a supported Pt catalyst for aromatic hydrogenation is enhanced by nitrogen compounds, but attenuated by chlorine compounds. Electronic effects are probably operating here: e.g., the sulfiding equilibrium can be changed; chlorine apparently weakening the Pt–S bond, as proposed by Dalla Betta and Boudart.[78]

Selective hydrogenation of acetylenes to the corresponding olefins (but not further to the paraffins) in C_2, C_3, and C_4 petrochemical streams is generally carried out on different types of supported Pd catalysts. In industrial practice, the plant is usually operated to maintain constant product specification. Hence, when the activity of the catalyst slowly declines due to coking, poisoning, or such reasons, the operating temperature of the catalyst bed is raised gradually to obtain the same conversion of the acetylenics in the feed stream. With palladium catalysts, however, one has to watch out that the pressure/temperature conditions are not reached for the α-to-β phase transformation of palladium hydride. Only the α phase is sufficiently selective for the semi-hydrogenation of acetylenes. This was demonstrated elegantly by Palczewska and her colleagues by conducting partial hydrogenation of acetylene in a combined flow-differential reactor–XRD chamber so that acetylene conversion and phase composition of a palladium catalyst could be followed simultaneously. Typical results are shown in Figure 9. With pC_2H_2 = 0.9 kPa as a constant, pH_2 was varied at 303 K. The catalyst, 3 wt % Pd on γ-Al_2O_3 with a mean Pd particle size of 18 nm, was in a state of metallic palladium or the α-Pd-H phase at point 1 (both in the phase diagram and in the XRD pattern); it was

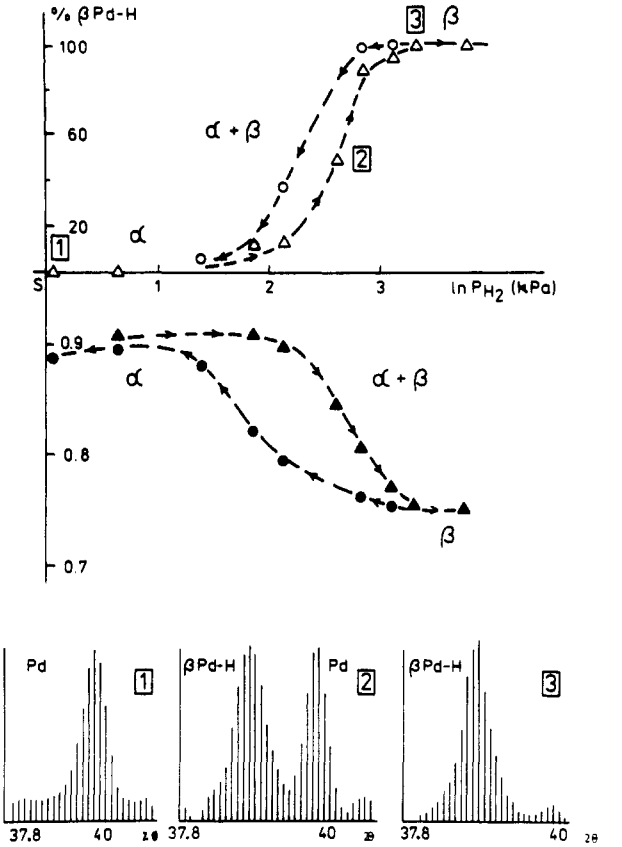

Figure 9. Relations between the phase composition of Pd–H system, expressed in percent β-Pd–H phase (upper half), and the selectivity of catalytic semi-hydrogenation of acetylene (lower half): (△, ▲) p_{H2} increasing; (○, ●) p_{H2} decreasing. The X-ray diffraction patterns 1, 2, and 3 were recorded using a step-by-step counting method; the figures were obtained after proper subtraction of background introduced by the support (from Palczewska,[79] copyright 1988 Marcel Dekker).

Table 5. Auger Analysis of the Outer Layer of Fresh and Deactivated Samples of a Pd/Alumina Catalyst for Selective Hydrogenation (Adapted from Bhasin[80])

	analysis, %								
	Mo	S	Ca	Pd	O	Cr	Fe	Co	Al
fresh cat.	3.3	1.5	0.7	1.3	55.8	0.7	0.0	0.2	36.5
deact cat.	0.0	1.4	0.9	0.3	70.1	0.0	13.7	0.4	13.2

selectively hydrogenating acetylene to ethylene with 90% selectivity. When pH_2 was raised to about 7 kPa, the phase transition of palladium into the β-Pd-H phase began; simultaneously the selectivity started decreasing (see point 2 at midpoint of this transition). At point 3, the phase transition was complete; at 100% β-H-phase, the selectivity had fallen to 70% (Palczewska[79]).

Bhasin[80] has reported a case from Union Carbide where a sudden loss of activity of the catalyst observed in the plant seemed to be caused by a change in feedstock a few days earlier. An Auger electron spectroscopic (AES) analysis of the fresh and spent catalysts gave very different compositions of the surface of the catalyst, as shown in Table 5. The outer surface of the spent catalyst contained such an accumulation of iron that it had covered about three-fourths of the Pd, all of the Mo and Cr, and even a good part of the Al of the alumina support. The presence of iron in small amounts is not a poison for the catalyst. But the masking of iron of the highly active Pd surface atoms and of the Cr/Mo promoter atoms had practically killed

the catalyst. The solution for this catalyst deactivation problem was obvious: do not use a feedstock containing so much iron.

In another case, selective semi-hydrogenation of methyl-, ethyl-, and vinylacetylenes in the crude C_4 stream of a petrochemical complex was being carried out in the liquid phase over a supported copper catalyst (cf. Couvillion[81,82]). After a few months of operation the catalyst was regenerated and then samples of catalyst were taken from the top, middle, and bottom of the catalyst bed. An EDX analysis showed the presence of about 3.0, 1.4, and 0.3 wt % S, respectively, on the samples. The feedstock processed was always reported as "sulfur-free". The feedstock flow in the reactor was upward so that any trapped sulfur from the feed should have exhibited an opposite profile in the bed: maximum S at the bottom and minimum at the top of the bed. A closer examination soon revealed the real truth. The "sulfur-free" specification of the C_4 stream only meant that S was below the level of detection (1 ppm) of the analytical method used. At 1 ppm S level, the quantity of C_4 stream passed over the catalyst during one cycle was still enough to deposit about 70 kg of S on the catalyst. This S content is of the same order as revealed by EDX analysis of the catalyst. Furthermore, although maximum S would be retained at the bottom of the catalyst bed and minimum at the top during the up-flow process, during the down-flow reduction (after the regeneration), H_2S was being stripped off from the catalyst. But part of this H_2S was inadvertently sent to the top of the bed *along with the recycled hydrogen from the reduction.* The H_2S reacts immediately with the freshly reduced copper catalyst. This accounts for the abnormal situation of a reverse sulfur profile from top to bottom of the reactor, although the feedstock flow initially deposited a bottom-to-top S profile. Once the reason for this pattern was understood, it was easy to stop the recycle of hydrogen during reduction and thus save the catalyst from accumulation of sulfur on it and prolong the cycle life (Menon[83]).

G. Selective Dehydrogenation

Another case of a mysterious and rapid catalyst deactivation involved a supported Pt catalyst used for selective dehydrogenation of *n*-paraffins to α-olefins (for subsequent alkylation with benzene to form biodegradable detergents). A comparative XPS analysis of fresh and deactivated catalysts showed an accumulation of fluorine on the surface of the latter. Hydrofluoric acid used as the alkylation catalyst had escaped upstream during a plant upset and had of course destroyed the catalyst (Prasada Rao[84]).

H. Fluid Catalytic Cracking

The fluid catalytic cracking (FCC) plant or "cracker" is often considered the heart of a modern petroleum refinery. In the FCC process, larger hydrocarbon molecules are cracked into smaller ones so that their boiling point and other properties are just in the desired range for LPG, naphtha, gasoline, diesel, cycle oils, middle distillates, heating oils, etc. There are about 300 FCC units in the world, nearly half of them in the United States. About 1 million tons of gas oil are cracked per day in the United States alone.

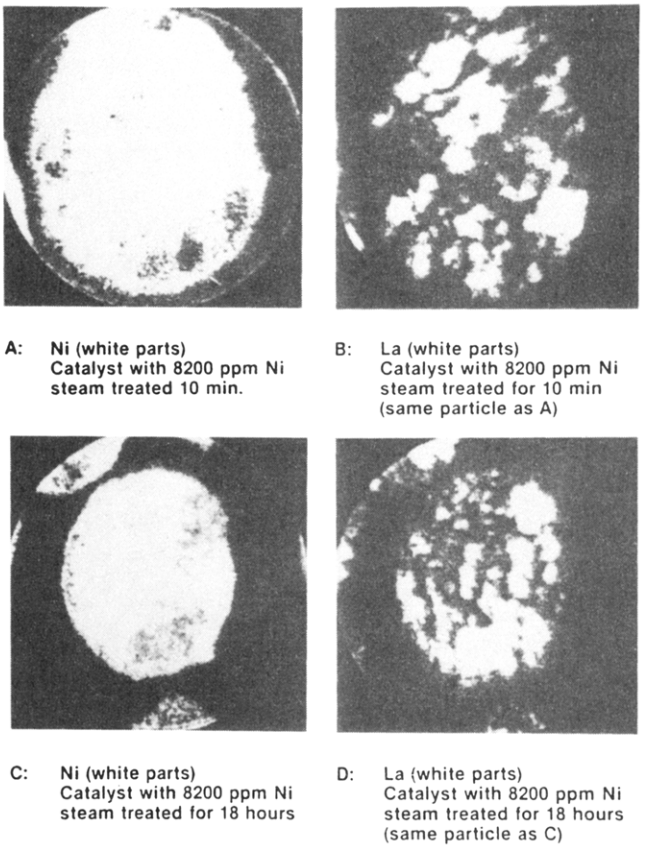

Figure 10. SIMS images of two FCC catalyst particles impregnated with nickel naphthenate (from Järås,[87] copyright 1982 Elsevier).

The rapid deactivation of catalysts by coke in catalytic cracking was so prevalent that it led to the development for the first time of fluidized-bed operations in FCC in the early 1940s. The peculiar problems of heavy-oil (resid) cracking and the adaptations of both the process and catalyst to face these problems in FCC have been presented by Otterstedt et al.[85] and Biswas and Maxwell[86] in earlier reviews. The gradual accumulation of Ni and V on the catalyst during hundreds of cracking–regeneration cycles has been studied extensively by several techniques. The disastrous consequences of Ni and V are quite different: Ni will produce more H_2, C_1–C_3 gases, and coke, all of which are undesired in the FCC process; V will destroy the crystal structure of the zeolitic molecular sieves in the catalyst. It was the use of secondary ion mass spectrometry (SIMS) which first showed clearly this throttling of zeolite by V. Using this technique, Järås[87] could locate the exact positions of (a) Ni and La and (b) V and La in FCC catalyst particles loaded with the corresponding metal naphthenate and examined before and after overnight steaming at 750 °C (Figures 10 and 11). Overnight steaming is the standard procedure for a laboratory simulation of what happens to the fresh catalyst in the plant after hundreds of cracking and regeneration cycles. The locations of the rare earth La in a single catalyst particle gives a direct mapping of where exactly the molecular-sieve crystallites are embedded in the matrix, because the rare-earth cations have been exchanged into the zeolite during the catalyst preparation. The SIMS mappings show that Ni is spread uniformly in the particle; it does not show any preference to accumulate on the zeolite before or after

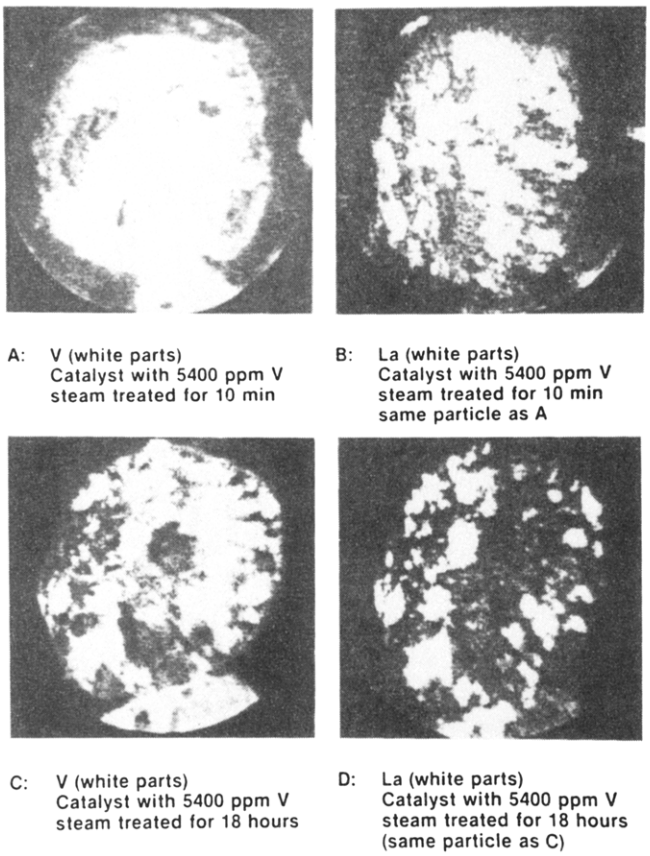

A: V (white parts) Catalyst with 5400 ppm V steam treated for 10 min

B: La (white parts) Catalyst with 5400 ppm V steam treated for 10 min same particle as A

C: V (white parts) Catalyst with 5400 ppm V steam treated for 18 hours

D: La (white parts) Catalyst with 5400 ppm V steam treated for 18 hours (same particle as C)

Figure 11. SIMS images of two FCC catalyst particles impregnated with vanadium naphthenate (from Järås,[87] copyright 1982 Elsevier).

steaming. Quite the contrary situation is seen with V: in the catalyst steamed overnight, the V has migrated preferentially to the La (i.e., zeolite) spots. More detailed SIMS studies on the deposition and migration of Ni and V in FCC catalysts have been reported recently by Leta and Kugler,[88] who illustrate the power of this technique to gain a novel insight of catalyst composition and performance and reaction pathways.

XPS studies[89] show that during cracking V is on the outside of catalyst particles. During regeneration, V_2O_5 starts migrating, because its melting point is only 690 °C, while the regenerator temperature can be 700 °C or higher. Furthermore, the steam formed in regeneration can react with V_2O_5 to form vanadic acid, which is quite volatile. The migration of V to the zeolite destroys the crystal structure of the zeolite. The mechanism of this structural collapse has been further elucidated by DTA/TGA techniques.[90]

Once the exact mechanisms are known as to how Ni distorts and V destroys the activity and selectivity of FCC catalysts, appropriate preventive measures can be taken. For Ni, the Phillips metal passivation process is widely applied: small quantities of Sb, added into the feed at ppm levels of an organometallic compound of Sb, will form an alloy with Ni. The surface enrichment of Sb on this Ni–Sb alloy effectively reduces the metallic area and thus minimizes the harmful effects of Ni on the equilibrium catalyst in FCC.

For V, there are at least two remedies. The greatest trouble is caused by V in its highest oxidation state as V_2O_5. If the regenerator can be operated under slightly oxygen-deficient conditions, or at least without any excess oxygen, much of the V will be in its lower oxidation state as V_2O_4 or V_2O_3. That is a practically harmless state of V. The second possibility is to use a vanadium trap, e.g., MgO, which forms magnesium vanadate, which is quite stable under FCC conditions. This renders the V nonvolatile and thus quite harmless. Simultaneous traps for both Ni and V are also being claimed nowadays, like oxides of Ca, Sr, Ba, Sn, and Ti and mixed oxides like titanates.[91]

I. Alkali Migration in Styrene Catalyst

Styrene is one of the most important monomers in modern petrochemical industry. The styrene process was developed in the 1930s independently and simultaneously by BASF in Germany and by Dow Chemical in the United States. The process is based on the dehydrogenation of ethylbenzene to styrene in the presence of superheated steam on a potassium-promoted iron oxide catalyst. Both the catalyst and the process have undergone several major improvements during the last 60 years. However, the migration of potassium promoter and its loss from the catalyst still remain as major problems.[92–94] Under the process conditions of 590–630 °C in steam, the alkali migrates in two dimensions: on the macroscale of the reactor, in the direction of process flow in the catalyst bed of 100–300 tons of catalyst and, on the microscale, from the exterior to the core of each catalyst pellet.[93] This migration and loss of potassium results in a serious loss of activity, selectivity, mechanical strength, and hence useful life of the catalyst. Hence many industrial and academic research groups are actively looking into this problem of alkali mobility and migration in the styrene catalyst. Only three detailed studies, carried out independently and almost simultaneously using different but often complementary approaches and techniques by three research groups in Germany, the Netherlands, and Sweden, will be described here.

Recently, Ertl and co-workers[52,95] at the Fritz Haber Institute, Berlin, Germany, in close collaboration with BASF, conducted very comprehensive studies on the styrene catalyst system. They used a variety of sophisticated and complementary experimental techniques: thermogravimetry under different atmospheres, both *ex situ* and *in situ* XRD, XPS, ultraviolet photoelectron spectroscopy (UPS), ion-scattering spectroscopy (ISS), extended X-ray absorption fine structure (EXAFS), and kinetic studies. From such an in-depth study, the Berlin group has established the various solid-state transformations occurring in the catalyst in its precursor, formation, activated-state, deactivation, regeneration, mechanical disintegration, and inactive states, as shown in Figure 12. The active state of the catalyst is believed to be an equilibrium between potassium ferrite, $KFeO_2$, and the phase $K_2Fe_{22}O_{34}$. Hydrogen, formed as product of the reaction, can play havoc here: it reduces the active catalyst to KOH and magnetite, Fe_3O_4. Once these phases are formed, segregation of the phases occurs, leading to a potassium-rich core and a potassium-depleted shell in each catalyst pellet or extrudate. These are not only inactive and nonselective phases but their mechanical strength is also much lower, leading to crumbling or crushing of the catalyst. There is also some coke formation, but this coke is readily gasified by steam, catalyzed by potassium. Hence this is a relatively

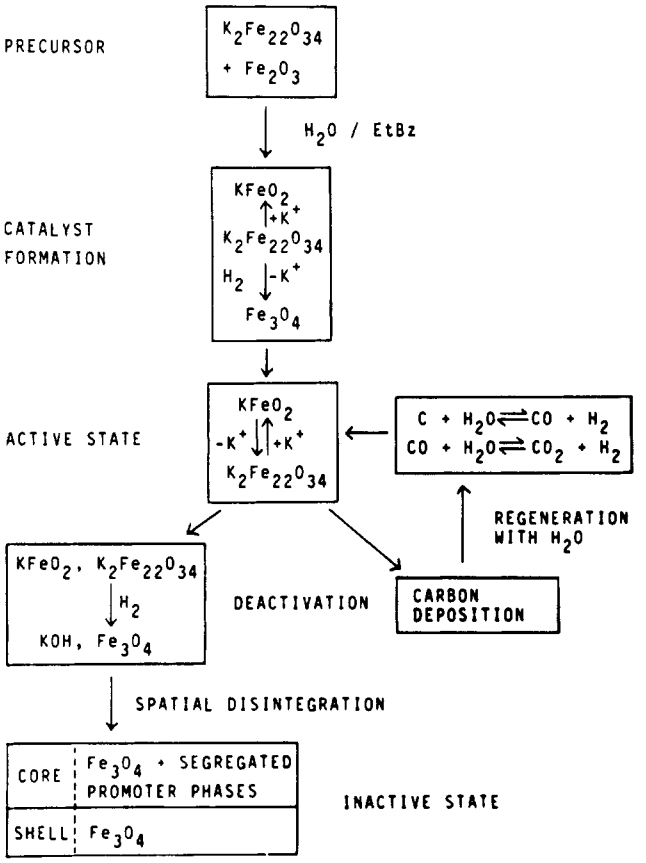

Figure 12. Schematic life cycle of a prototype styrene catalyst (iron oxide + potassium oxide) without any other promoter oxide additives (proposed by Muhler et al.,[95] copyright 1990 Academic Press).

harmless and reversible deactivation. On the other hand, the reduction of the catalyst and the consequent phase segregation lead to irrevocable damage and destruction of the catalyst. The role of other oxides, added as promoters, is to retard the rate of the unwanted deactivating solid-state transformations. This detailed understanding of the chemistry of the life cycle of the styrene catalyst led to the development by BASF of a new generation of still better industrial catalysts for the styrene process (Büchele[96]).

At the University of Utrecht, Geus and co-workers, working in collaboration with Dow Chemical, have studied ways and means to overcome the detrimental effects of potassium migration in the styrene catalyst by applying the iron oxide phase onto a preshaped magnesia support (cf. Stobbe[97] and Stobbe et al.[98-101]). XRD, TPR, high-field magnetic measurements, and kinetic studies were used to characterize the supported-catalyst system. In the fresh catalyst without potassium, the iron oxide is present[98] as highly dispersed magnesium ferrite, $MgFe_2O_4$. This unpromoted catalyst shows low dehydrogenation activity and selectivity; it also rapidly deactivates due to the formation of a carbonaceous layer on the catalyst surface.[99] Using thermomagnetic analysis, it was shown that the $MgFe_2O_4$ phase is reduced during the dehydrogenation to form a solid solution of FeO in MgO with a surface layer of Fe_3O_4.

On promotion with potassium carbonate, the magnesium ferrite reacts to form potassium monoferrite, $KFeO_2$, above 650 °C (Stobbe et al.[100]). The potassium-promoted supported catalyst shows[101] a considerably

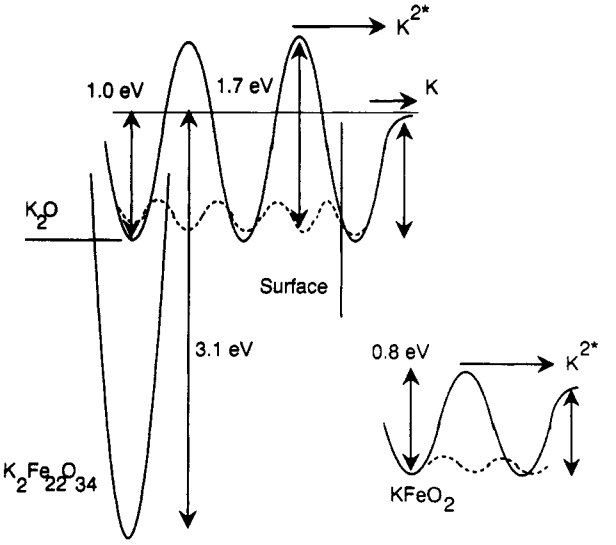

Figure 13. Energy diagram for the potassium promoter in the iron oxide catalyst for the styrene process (from Engvall et al.,[104] copyright 1991 Elsevier).

higher activity and selectivity than those of the unpromoted one, comparable to those of the unsupported commercial catalysts of today. Under dehydrogenation conditions, $KFeO_2$ is not reduced. It was confirmed from kinetic measurements that $KFeO_2$ is the active phase of the catalyst during dehydrogenation; this is the hypothesis already proposed earlier by Hirano[102] and Muhler et al.[95] Although $KFeO_2$ shows high dehydrogenation activity and selectivity, Stobbe et al.[101] have shown that it is not sufficiently active in catalyzing carbon gasification to suppress coking entirely. They conclude that complete suppression of coking requires the additional presence of highly dispersed potassium carbonate.

At Göteborg, Holmlid, Menon, and their co-workers,[104-107] in collaboration with Chemetall GmbH, studied the emission of potassium species from fresh and used commercial styrene catalysts at 600–800 °C, using ultrahigh vacuum (UHV) and molecular-beam techniques. They used a quadrupole mass spectrometer, field ionization, surface ionization, and field-reversal kinetics as detection techniques. By suitable combination of these techniques, the emission from the catalyst of potassium as atoms, ions, clusters, and excited species (the so-called Rydberg states) could be identified and measured. Their separate concentrations, angular distributions, and activation energies for desorption could be determined. From such studies, and taking into account the detailed mechanism of the solid-state transformations proposed earlier by Ertl's group[95] and shown in Figure 12, an energy diagram for the potassium promoter in the iron oxide catalyst for the styrene process could be constructed[104] (Figure 13).

The potassium loss from the industrial styrene catalyst at process temperatures (about 600 °C) and above, but under UHV conditions, occurs in the form of not only K atoms but also as excited states, K*, doubly excited states, K^{2*}, and as clusters, K_n. This suggests that the behavior of the alkali loss from the catalyst is much more complicated than hitherto realized. The operational stability of the catalyst under styrene process conditions can perhaps be enhanced by the addition of other oxides (e.g., oxides of Ca, La, Ce, V,

and W) as promoters, which can play a double role: (a) retard the undesired catalyst-deactivating solid-state transformations shown in Figure 12, proposed by Muhler et al.,[95] and (b) raise the temperature threshold for the thermal desorption of K species from the catalyst, as proposed by Holmlid et al.[105] A comparative study by Engvall et al.[104] of two commercial styrene catalysts showed that the better catalyst had indeed a much higher temperature threshold for the desorption of K, both as K atoms and as K^{2*} excited species. In this respect, such molecular-beam study under UHV conditions is proving to be a valuable fingerprint and possibly even an accelerated life test for industrial styrene catalysts.

Using scanning electron microscopy (SEM) and scanning Auger microprobe (SAM) to study fresh and used (for 9 months in the plant reactor) styrene catalysts, Lundin et al.[107] could show spots or patches on the used catalyst surface having the chemical composition of potassium ferrite, $KFeO_2$. There is already a consensus view, emerging from the almost parallel and independent researches of Hirano[102] in Japan, Muhler et al.[95] in Germany, and Stobbe et al.[98-101] in the Netherlands, that potassium ferrite is the active phase on the styrene catalyst under actual process conditions. The identification by Lundin et al.[107] of the ferrite on the surface of the catalyst, taken out of the plant reactor after 9 months of operation, supports this consensus view. It is also a positive testimony that some of the modern surface-science techniques can be applied directly to study the surface of real industrial catalysts.

J. Reconstruction of Acrylonitrile Catalyst

The ammoxidation of propylene to acrylonitrile is one of the most successful processes in the present-day petrochemical industry. In the 1960s this process, developed by Sohio, displaced almost completely the older energy-intensive process based on the direct combination of acetylene with hydrogen cyanide (both of which were then produced by the electric-arc process). This is also a classical example for the cheaper and safer olefin-based processes of the 1960s which swept away the more hazardous acetylene-based processes of the preceding three decades.

$$C_2H_2 + HCN \rightarrow CH_2{=}CHCN$$

(old process)

$$CH_2{=}CHCH_3 + NH_3 + {}^3/_2O_2 \rightarrow CH_2{=}CHCN + 3H_2O$$ (Sohio process)

The Sohio process is based on a bismuth–molybdate type catalyst, supported on silica, and is used in fluidized-bed operation. Several generations of better and still better catalysts have been brought on the market by Sohio, Asahi, Nitto, and other companies. Many of the later-generation catalysts are typical cocktails: multicomponent molybdates with other promoter (e.g. Fe, Co, Ni, Se, Sb, and P) oxides, alkali, and other additives, and the usual 50% silica.

Prasada Rao and Menon[108] employed (a) thermogravimetry, (b) DTA, (c) X-ray diffraction, (d) infrared spectroscopy, (e) ESR, (f) Mössbauer spectroscopy and (g) XPS to characterize silica-supported multicomponent molybdate catalysts before and after use in the ammoxidation of propylene. Techniques a and b showed the absence of free oxides in the catalyst samples, c and d the presence of various molybdate phases in the system, e and f the reduction of Fe^{3+} in the fresh catalyst to Fe^{2+} in the used catalyst, while *XPS alone could show the radical changes in the composition of the catalyst surface on exposure to actual reaction conditions.* Hardly any change was noticed when the catalyst was exposed to the same temperature as in the reaction but in the absence of the reactants. The percentage change in the surface composition of the used catalyst relative to that of the fresh one is shown in Figure 14. The surface of the used catalyst is enriched with Mo, Bi, Fe, and O_I (oxygen of the metal–oxygen bond) and is depleted of Co, Ni, Si, and O_{II} (oxygen of the Si–O bond). Fortunately, these benevolent surface reconstructions only made the catalyst active, but they show how easy it is to deactivate the catalyst by extraneous factors or poisons in the feed stream.

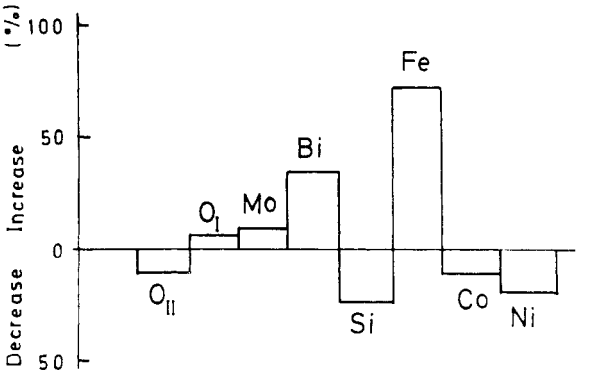

Figure 14. Relative percentage change in surface composition (from XPS) of a multicomponent molybdate catalyst, compared to that of the fresh one (base line), after us in ammoxidation of propylene to acrylonitrile (from Prasada Rao and Menon,[108] copyright 1978 Academic Press).

K. Iron Molybdate for Methanol Oxidation

Molybdates form a very important group of catalysts for oxidtion, ammoxidation (see the previous paragraph), hydrotreating, olefin metathesis, etc. Iron molybdate is prominent for the oxidation of methanol to formaldehyde. In the 1960s, it was also in the third-generation catalyst for the ammoxidation of propylene to acrylonitrile. When present alone, ferric molybdate is active for methanol oxidation, but it is not selective for formaldehyde, and it also deactivates rapidly. This deactivation seems to be caused by a slow reduction of ferric molybdate to ferrous molybdate and various lower oxides of the type MoO_{3-x}. One way to overcome this deactivation is to incorporate another oxide, antimony oxide, in methanol oxidation. Xiong et al.[109] have investigated the role of Sb_2O_4 in preventing the deactivation of iron molybdate, using BET surface area, XRD, XPS, TEM/SEM, Mössbauer spectroscopy, and catalytic activity studies (for oxidation of ethanol to acetaldehyde and of isobutane to methacrolein). When iron molybdate is used alone as the catalyst, after 30 h of catalytic reaction, the catalyst surface contains spots with Mo only, as shown in the electron micrograph of Figure 15; when another oxide like Sb_2O_4 is present, no spots containing reduced Mo only can be detected.

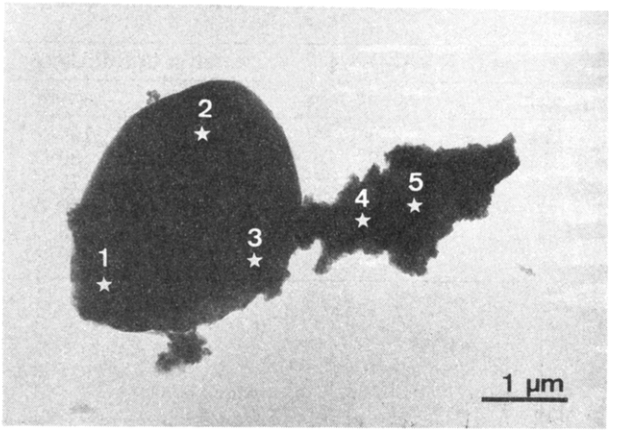

Figure 15. Transmission electron micrograph of pure iron molybdate catalyst after 30 h of catalytic oxidation on it. The Mo/Fe ratios at the indicated points on the surface are 1, 1.98; 2, 1.88; 3, 1.71; 4 and 5, only Mo (from Xiong et al.,[109] copyright 1991 Elsevier).

From these and other results, the authors conclude that the role of Sb_2O_4 is to supply spill-over oxygen by the remote-control mechanism forwarded by Delmon.[110] This flow of surface oxygen prevents the excessive reduction of $Fe_2(MoO_4)_3$ and thus retards or avoids the nucleation of reduced pure molybdena phases.

L. Copper Catalyst for the Acrylamide Process

The hydrolysis of acrylonitrile to acrylamide is an important industrial process:

$$CH_2{=}CHCN + H_2O \rightarrow CH_2{=}CHCONH_2$$

The preferred catalyst for this process is Raney copper because it is selective for the hydrolysis and because the deactivated catalyst can be regenerated by a simple alkali wash with NaOH solution, similar to that used to activate the Raney copper alloy. Lee et al.[111] studied the deactivation of Raney Cu and silica-supported Cu for the acrylamide process. An initial rapid deactivation was observed due to the fouling of the surface by a polymer produced from acrylamide; at least a part of the polymer is formed by a process involving the catalyst. A second deactivation process, caused by interaction of the catalyst with oxygen (dissolved in acrylonitrile), was also observed. This deactivation was very significant with supported catalysts where the small Cu particles were oxidized more easily than the larger ones as in Raney Cu. The activity of the catalyst after the initial deactivation was found to depend on the size of the pores in the catalyst. Hence the catalyst performance could be improved by larger Cu crystallites (lower Cu dispersion) and larger average pore diameters (>20 nm).

M. Hydrogenation of Nitrobenzene to Aniline

Dvorak et al.[112] studied the deactivation of a supported Cu catalyst for the industrial-scale hydrogenation of nitrobenzene to aniline. Four distinct causes for catalyst deactivation could be identified here: (1) contamination of the catalyst surface by macromolecular carbonaceous deposits; (2) poisoning of the active copper sites by chlorine and sulfur compounds, present as trace impurities in nitrobenzene; (3) sintering of copper crystallites present initially; and (4) mechanical crumbling of the catalyst pellets, leading to increased pressure drop and ultimately reactor plugging.

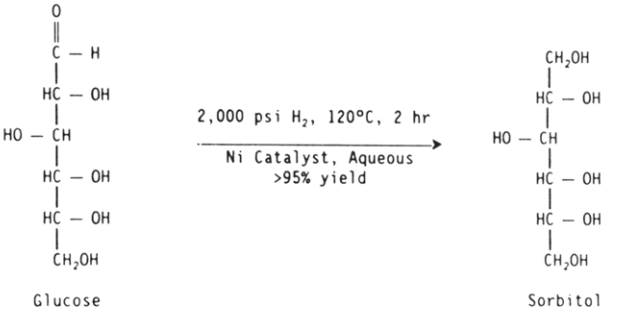

Figure 16. Hydrogenation of glucose to sorbitol (from Arena,[114] copyright 1992 Elsevier).

The support composition, the presence of poisons, and the concentration of 1,3-dinitrobenzene in the feedstock have major influence on coke deposition. The catalyst sintering occurs nearly exclusively at the beginning of the operation cycle. The exact mechanism of pellet crumbling is still not known. But, because this mechanical breakdown occurs only in a relatively narrow top layer of the catalyst bed, one practical solution to the pressure-drop problem is to remove the finer catalyst particles from the top layer by vacuum suction. Such a simple procedure could prolong the catalyst life by up to 40%.

N. Titanium Silicalite

During the 1980s titanium silicalite (TS) emerged as a powerful new catalyst for liquid-phase selective oxidations in the presence of hydrogen peroxide as the oxidizing agent. Petrini et al.[113] have studied deactivation phenomena of TS in the ammoxidation of cyclohexanone to its oxime. The catalyst was characterized by chemical analysis, thermogravimetry, IR and UV–vis spectroscopy, XRD, gas adsorption, and a standard activity test. Three main deactivation processes have been identified: (a) slow dissolution of the framework with accumulation of Ti on the external surface of the remaining solid, (b) direct removal of Ti from the framework, and (c) pore filling by the byproducts of the catalytic reaction.

O. Ru Catalysts in Glucose Hydrogenation

Arena's study[114] on catalytic hydrogenation of glucose to sorbitol is an outstanding example to show how a systematic in-depth study can lead not only to trouble-shooting in catalyst deactivation but also to the design of better industrial catalysts and catalytic processes. The hydrogenation of glucose to sorbitol is shown in Figure 16. Since sorbitol product specifications for food use allow only <0.3% glucose, 99.7% or higher conversion is a strict goal. Alumina-supported Ru catalysts can give such conversion, but slow catalyst deactivation was an attendant problem. The changes in the catalyst are evident from analysis of fresh and spent catalysts, shown in Table 6; conversion from 100% to 99% was already unacceptable due to the 99.7% product purity needed. Factors contributing to slow catalyst deactivation are (a) slow agglomeration of Ru particles with a loss of Ru-metal surface area, (b) transformation of the support alumina, (c) buildup of iron, leached out from the reactor walls, (d) sulfur, and (e) gluconic acid,

Table 6. Physical Characterization of Fresh and Spent Supported Ru Catalysts for Hydrogenation of Glucose to Sorbitol (from Arena[114])

	catalyst A, $Ru/Ti-Al_2O_3$		catalyst B, Ru/Al_2O_3		catalyst C, Ru/Al_2O_3	
	fresh	spent	fresh	spent	fresh	spent
Ru crystallite size (Å)	<80	120	114	230	168	154
Al_2O_3 crystallinity (%)	43	48	42	70	75	80
BET surface area (m^2/g)	179	149			67	72
pore vol for >30 Å (mL/g)					0.63	0.47
average pore diam >30Å (Å)					295	273
time on stream (h)		720		400		400

formed by Ru-catalyzed oxidation of glucose by oxygen dissolved in the reactants.

Once these causes of catalyst deactivation were pin-pointed, precautionary or remedial measures were obvious: (a and b) Physical changes of both Ru and the alumina support could be minimized by lowering the severity of the process: by developing a more active catalyst, still with the same Ru loading, the process temperature could be lowered from 120 to 104 °C. (c) A Teflon lining of the reactor wall eliminated iron leaching from the wall and catalyst poisoning by the iron. (d) A guard bed could be used to trap off all sulfur compounds in the feedstock. (e) By removing dissolved oxygen from glucose and maintaining a nitrogen blanket in the liquid reservoir tanks for glucose, Ru-catalyzed oxidation of glucose to gluconic acid was effectively suppressed. Thus, gluconic acid poisoning of the catalyst and gluconic acid as an impurity in the product were both eliminated.

The net result from these preventive measures was a stabler catalyst and an improved process for hydrogenation of glucose to sorbitol.

P. Coke, Sulfur, and Metals on Hydrotreating Catalysts

Hydrotreating is the common term in petroleum industry to refer to a variety of processes involving double-bond saturation, hydro-desulfurization, hydro-denitrogenation, and hydro-demetalation. In the wake of the energy crisis from 1973 onwards, it became increasingly necessary for petroleum refineries to process heavier and heavier oil fractions. The hydrotreating capacity has now reached about half of the installed crude-petroleum refining capacity. Hydrotreating catalysts are usually γ-alumina-supported oxides of Mo or W, promoted with oxides of Co and/or Ni and also containing some phosphate. Under process conditions, the active oxides are converted to the sulfides. These catalysts, if properly designed, can take up a high load of coke, sulfur, and metals from the heavy or resid feedstock; they undergo very slow deactivation in the course of several months upto a few years. Simpson[115] has reported the coke, sulfur, and metal profiles in a demetalation catalyst after an extended testing. The used catalyst was taken out of the reactor in 11 consecutive sections and analyzed separately. The carbon (coke) level increased, and the sulfur and metals levels decreased, from top to bottom in the direction of process flow in the bed, as shown in Figure 17. The level of deposited metals (V + Ni + Fe) ranged from about 110% by weight of the fresh catalyst at the top of the bed to about 15% at the bottom in a fairly linear fashion (Figure 18). The average deposited metals level was 52 wt % of the fresh catalyst. The

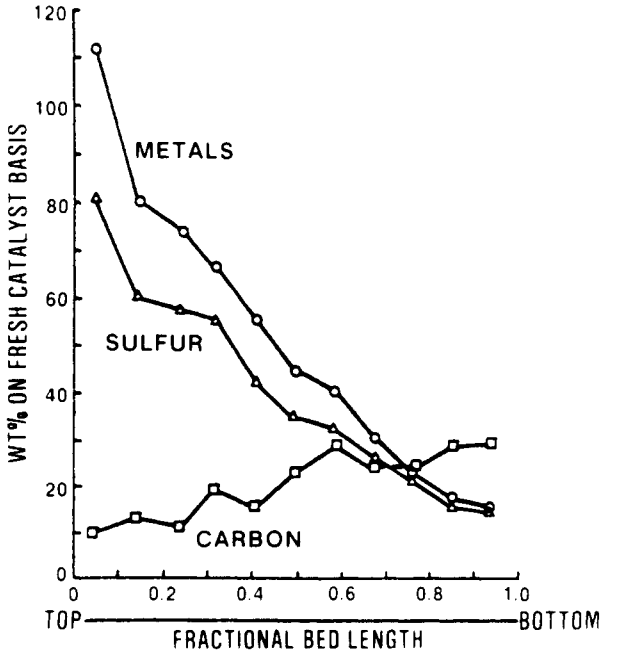

Figure 17. Profiles of coke, sulfur, and metals in the spent demetalation catalyst bed (from Simpson,[115] copyright 1991 Elsevier).

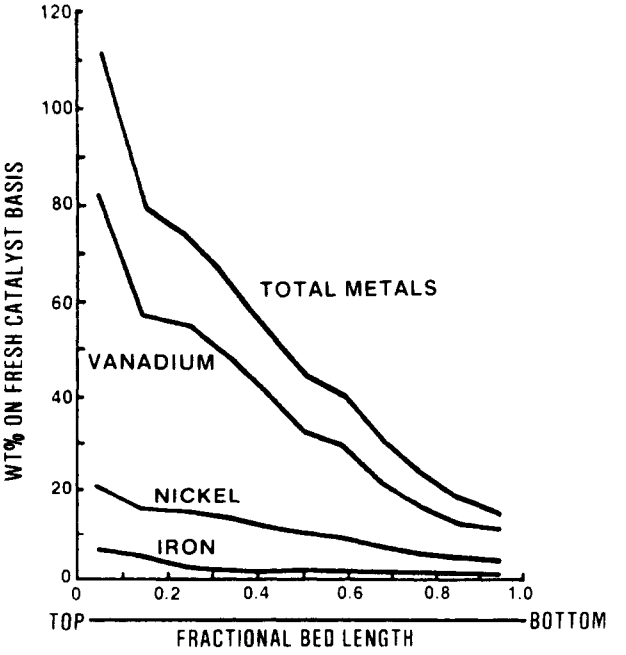

Figure 18. Profile of component metals V, Ni, and Fe on the spent demetalation catalyst (from Simpson,[115] copyright 1991 Elsevier).

apparent stoichiometric ratio of metals to sulfur ranged from 1:1 at the top of the bed to 1:2 at the bottom. Electron microprobe line scans (Figure 19) show that

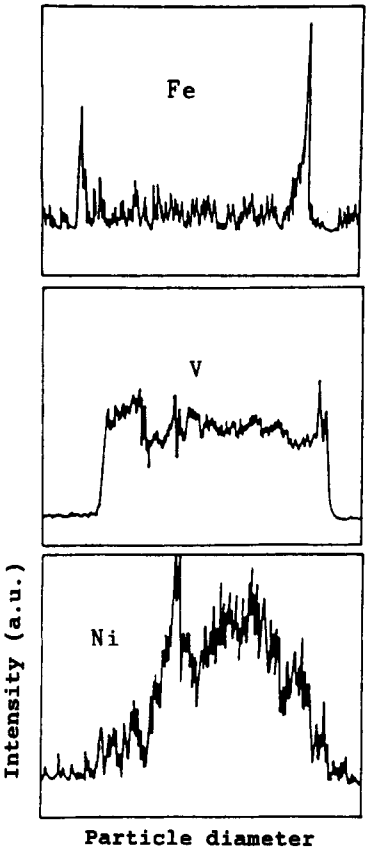

Figure 19. Typical line scan for V, Ni, and Fe in catalyst particles taken from the top of the spent demetalation catalyst bed (from Simpson,[115] copyright 1991 Elsevier).

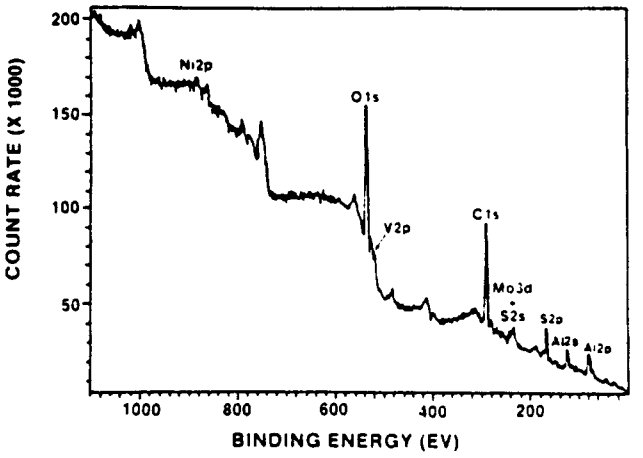

Figure 20. XPS scan of used hydrotreating catalyst (powdered) taken from the top (inlet) of the catalyst bed (from Simpson,[115] copyright 1991 Elsevier).

V tends to deposit fairly uniformly throughout the catalyst particles, especially at high loadings. Ni exhibits a "reverse rinding" effect, where the concentration is higher in the interior of the particles than on the outside. Fe exhibits a very high rinding effect.

Simpson[115] also employed X-ray photoelectron spectroscopy (XPS or ESCA) to examine the samples taken from different bed heights, analyzing both the outer surface of the catalyst pellets and the powder after pulverizing the pellets. Figure 20 shows typical XPS data for a powdered catalyst sample taken from the top of the bed. The composition of the outer surfaces of all samples was similar. The analysis of the powdered samples, however, reflected the concentration gradients

Table 7. Summary of XPS Results on Used Hydrotreating Catalysts (from Simpson[115])

element	chemical form, as inferred from XPS data
coke	Mainly amorphous carbonaceous material; only C–H and C–C bonds indicated
Mo	As MoS_2 or MoO_2; MoO_3 not detected
Ni	As $NiAl_2O_4$, $NiMoO_4$, $NiSO_4$; Ni_2S_3 or NiO also in top samples
V	Predominantly as V^{5+} sulfide or oxide (517 eV); also as VS or $MoVS_4$ species (513.5 eV)
Fe	As Fe^{3+}
S	Both as sulfide (162.5 eV) and sulfate (169 eV) (possibly from air exposure after unloading)

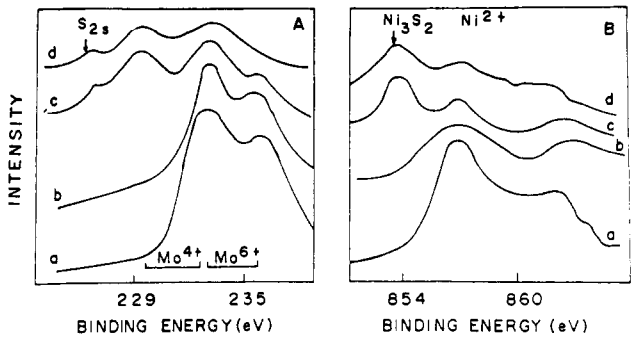

Figure 21. X-ray photoelectron spectra of Mo_{3d} (A) and Ni_{2p} (B) for lube hydrotreating catalysts: (a) fresh catalyst as oxide, (b) used RGD-2 as oxide, (c) sulfided fresh catalyst and (d) sulfided RGD-2 (from Ramaswamy and Sharma,[116] copyright 1991 Elsevier).

observed for the various elements by emission spectroscopy (Figures 17 and 18): carbon increases while V, Ni, and S decrease from the top to the bottom (from inlet to exit) of the bed. This detailed XPS study led to the interesting inferences summarized in Table 7. Simpson suggests that nearly all of the nonsupport elements compete with Al for the available oxygen, implying that metals incorporation in the support could be a mechanism for support degradation and destruction of the catalyst. Furthermore, some Mo was also detected on the surface of *all* of the catalyst particles, suggesting accessibility to the reactants of some Mo sites even when high levels of metal deposits are on the catalyst surface.

Ramaswamy and Sharma[116] have reported a detailed examination of two regenerated Ni–Mo–alumina catalyst samples withdrawn from a lube hydrofinishing reactor after 8 and 12 years of operation (after the fourth and sixth regeneration and designated as RGD-1 and RGD-2 respectively). The decrease in surface area, pore volume, and molybdena dispersion and the decline in thiophine hydro-desulfurization activity of the samples in relation to the fresh one are not related to the deactivation of the catalyst. TPR results point to more difficult-to-reduce Ni/Mo species at low temperatures in the regenerated samples. Figure 21A shows Mo_{3d} X-ray photoelectron spectra for the fresh catalyst in its oxide form (a) and sulfided form (c) and the used RGD-2 sample in its oxide form (b) and sulfided form (d). The position of Mo^{4+} species, attributed to MoS_2-like species, decreased significantly on the outer surface layer in the RGD-2 sample, compared to that in the sulfided fresh sample. Figure 21B shows Ni_{2p} spectra of the same two catalyst samples in their oxide and sulfided forms. The $Ni_{2p3/2}$ peak appeared at binding energy 356.8 eV for the oxide catalyst. On sulfiding, this peak

Table 8. Surface Composition of Fresh and Regenerated Lube Hydrotreating Catalysts after 8 (RGD-1) and 12 Years (RGD-2) of Operation in the Plant (XPS Data from Ramaswamy and Sharma,[116] Copyright 1991 Elsevier)

	relative intensity in atomic ratio to Al							
catalyst	Al	C	O	Ni	Mo	S	Fe	Ni/Mo
fresh oxide	100	64	164	2.1	5.1			0.41
RGD-1 oxide	100	53	151	1.2	3.5			0.34
RGD-2 oxide	100	50	112	0.5	2.5		11	0.22
sulfided fresh	100	85	142	1.9	5.3	11		0.36
sulfided RGD-2	100	123	146	0.5	3.6	12	10	0.14

is shifted to 854.0 eV, which was assigned to Ni_3S_2. A comparison of the spectra of the fresh and RGD-2 sample shows that both Ni^{2+} and Ni_3S_2 species are present in lower concentrations in the RGD-2 sample, irrespective of the state (oxide or sulfide) of the catalyst. Table 8 shows the surface compositions of the fresh catalyst and its sulfided form and RGD-1 as oxide and RGD-2 both as oxide and as sulfided. For the two regenerated catalysts, the Mo/Al ratios progressively decrease, RGD-2 having only half the value of that for the fresh catalyst; this indicates the steady loss of Mo from the exterior of the catalyst during prolonged use in the process or during regenerations. Chemical analysis, however, showed only a small decrease of MoO_3 from 14.3 to 13.9 and 12.5 wt % after 8 and 12 years of operation. As far as Ni is concerned, XPS data show a progressive decrease in the Ni/Mo ratio of the two RGD samples compared to the fresh one, but chemical analysis showed no loss of Ni from the catalyst. These results suggest that there is a slow migration of Ni (and Mo) to the bulk of alumina, probably toward the subsurface layer in the course of four to six regenerations of the catalyst. This is supported by the increasing difficulty for reduction of the catalysts observed during TPR runs of these samples. In hydrofinishing of lubricating oils, both the hydro-desulfurization by Mo and the hydro-denitrogenation by Ni are important. The progressive decrease in Ni/Mo ratio points to a slow deactivation of the catalyst with every cycle during the life of the catalyst.

Extensive investigations are also going on to develop methods to regenerate hydrotreating catalysts when they are deactivated by coke and metals (mainly Ni and V). Clark et al.[117] discuss two regeneration methods: (1) decoking without removal of contaminant metals and (2) removal of contaminant metals, followed by decoking. For each method, the regenerated catalyst was evaluated on the basis of several criteria, including activity, catalyst properties, and physical integrity including attrition resistance. Both regeneration methods were effective in restoring catalytic activity; however, the attrition resistance in both cases was still inadequate.

Q. Oxidative Coupling of Methane

For the oxidative coupling of methane to C_2+ hydrocarbons, Li-doped MgO is a popular catalyst above 700 °C, but mostly in quartz reactors. Since almost all metals have high activity for hydrocarbon combustion at these temperatures, Alonized 316 stainless steel reactors were tried for oxidative coupling of methane by Phillips and Eastman.[118] Severe corrosion of the portion of the reactor in contact with the catalyst bed was observed. Cr was leached out from the stainless steel of the reactor wall and deposited on the catalyst, where it catalyzed the complete combustion of methane to CO and CO_2. Since Alonized tubes used in other reactions have not shown such corrosion effects, these changes seem to have been caused by the migration of Li from the catalyst on to the reactor wall in contact with it. Electron probe microanalysis (EPMA or EDX) of the metal composition of the cross sectional traverse of the reactor tube wall above the catalyst bed and below it shows the restructuring of the reactor wall occurring *as a consequence* of the catalytic reaction. Such corrosion of reactor walls may also be expected from other alkali-promoted catalysts at high temperatures, e.g., the iron oxide catalyst for the styrene process, operating at 590–620 °C in the presence of super-heated steam, or the supported Ni catalyst for steam-reforming of hydrocarbons at 800–900 °C.

The deactivation of Li-promoted magnesia in oxidative coupling of methane was studied by Mirodatos et al.,[119] using surface-area measurements, TEM, XRD, DTA, and atomic emission spectroscopy for Li, and atomic absorption spectroscopy for Mg. These studies show the following. (1) Different modes of catalyst sintering have to be considered according to the temperature and the prevailing atmosphere: (a) sintering via the liquid Li_2CO_3 phase at high temperature and (b) sintering under the influence of H_2O and CO_2 in the course of the reaction. (2) Two different types of catalyst deactivation can occur with respect to the two sintering processes. (3) Optimum catalyst performance is obtained when a tight interface between Li_2CO_3 and MgO phases is achieved, after a treatment allowing the melting of the alkali salt.

R. Fischer–Tropsch Synthesis

Renewed interest in Fischer–Tropsch (FT) synthesis and the emergence of a new C_1 chemistry were two of the results of the oil crisis of the 1970s. Lower oil prices from the mid-1980s have reduced the research efforts in this area. Catalyst-deactivation phenomena by poisoning (by sulfur or halogens), fouling ("coke"), sintering, and other solid-state transformations have all been studied for various types of FT catalysts. In view of the extensive literature readily available on FT synthesis and the new C_1 chemistry, only references to a few reviews[120–123] are cited here.

S. Synthesis of Higher Alcohols

The stability of two ZnO/Al_2O_3-supported Cu/Co catalysts for higher alcohol synthesis from synthesis gas (CO + 2 H_2) was studied by Xu and Scholten.[124] One catalyst was promoted with KOH and the other was not. The two catalysts were tested in a Berty reactor at 280 °C and a total pressure of 50 bar for 1600 and 4200 h, respectively. The fresh and used catalysts were examined by X-ray diffraction, elemental analysis, total (BET) and specific-metal surface areas, thermogravimetry, and TPR. These studies showed that the catalysts were deactivated by more than the three well-known and common causes, namely coking, poisoning, and sintering. The unpromoted catalyst lost 17% of its total surface area and 56% of its free-metal (of Cu and

Co) surface area during the 4200 h on stream. The KOH-promoted catalyst fared still worse: it lost 49% of its total surface area and 76% of its free-metal area in 1600 h. Deposition of coke and formation of cobalt carbide were also detected on the deactivated catalyst samples. Total structural disintegration of the catalyst occurred simultaneously due to two other causes: (1) the gradual split-off of ZnO from zinc aluminate spinel, followed by sublimation of zinc from the reduction of ZnO, and (2) the slow leaching out of alkali (Na and K) by water, which is a byproduct of the reaction. There is no possibility of a regeneration for such a totally disintegrated and deactivated catalyst.

T. Woven versus Knitted Pt–Rh Gauze Catalysts for Nitric Acid

The manufacture of nitric acid is based on catalytic oxidation of ammonia to NO/NO_2, followed by absorption of NO_2 in water:

$$4NH_3 + 5O_2 \rightarrow 4NO + 6H_2O$$

$$2NO + O_2 \rightarrow 2NO_2$$

$$3NO_2 + H_2O \rightarrow 2HNO_3 + NO$$

The ammonia-oxidation stage uses a catalyst pack containing up to 36 gauzes of a Pt–Rh alloy. One of the serious problems in the use of the gauze catalyst is the Rh enrichment occurring as a result of the oxidation of Pt to PtO and the volatilization of PtO from the catalyst surface. Rh also oxidizes but does not volatilize so readily. When a 10% Rh–90% Pt alloy is in use, Pt is lost about 20 times faster than Rh, leading to an enrichment of Rh; the final composition can then reach 13% Rh–87% Pt.

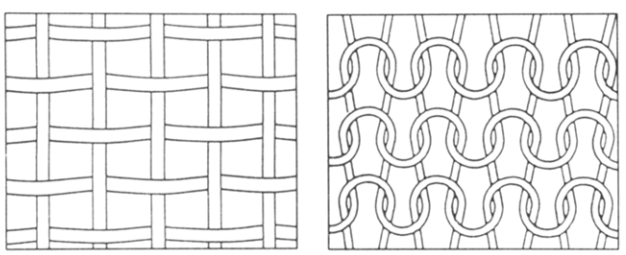

Figure 22. Structures of woven (left) and knitted (right) Pt–Rh gauze catalysts for nitric acid manufacture. The more open structure of the knitted material is compensated for by its bulky three-dimensional nature (from Horner,[125] copyright 1993 Johnson Matthey, London).

Since 1990, in nitric acid plants knitted Pt–Rh alloy gauzes are gaining ground over woven ones, which have been in use for the last 80 years. The structures of woven and knitted gauze catalysts are shown in Figure 22. The more open knitted structure offers less resistance to gas flow. This enables the reaction to occur further into the gauze pack, ensuring a more even temperature profile across the whole pack. This improved spreading of catalytic activity in the gauze pack, in turn, reduces the metal loss per gauze, with a resultant drop in the formation of RhO_2 (Horner[125]).

Another major factor contributing to the enrichment of RhO_2 on the surface is the presence of contaminants, particularly iron. The improved gas flow through the knitted gauzes results in less solid particles being trapped and hence less RhO_2 formed due to iron contamination. With equal impurity levels, the accumulation of iron is only 0.06% on the knitted gauze, contrasted to 0.36% on the woven gauze; the respective Rh contents on the surface are 12.1 and 18.7%. After a typical production run of 11 345 tons of nitric acid, the metal losses from knitted and woven gauzes were 0.032 and 0.042 g/ton of nitric acid produced and the Rh concentrations on the surface were 14.2 and 34%, respectively. After use in ammonia oxidation, both knitted and woven gauzes show restructuring of the surface. Fragile "cauliflower"-like formations grow on both types of catalyst (Figure 23), but on the knitted gauzes, the structural rearrangement is widely dispersed throughout the catalyst pack, leading to a more even temperature distribution, less mechanical damage, and reduced Pt loss, as compared to the woven gauze.[125]

U. Claus Catalysts

In petroleum refineries, sulfur compounds in the oil fractions are removed by various hydro-desulfurization processes. These processes convert organically-bound sulfur to H_2S, which has then to be oxidized to elemental sulfur. In modern refineries, H_2S is converted to sulfur by the Claus process on an alumina catalyst: first a

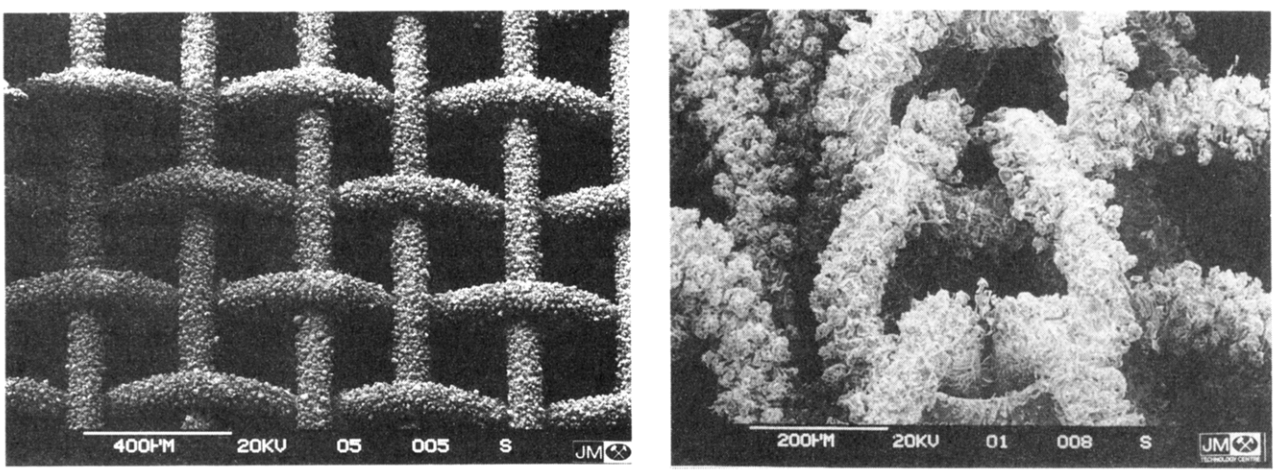

Figure 23. Scanning electron micrographs of restructuring on woven (left) and knitted (right) Pt–Rh gauze catalysts, used in the manufacture of nitric acid (from Horner,[125] copyright 1993 Johnson Matthey, London).

part of the H_2S is oxidized to SO_2, then the remaining H_2S is directly reacted with SO_2:

$$H_2S + 1.5O_2 \rightarrow H_2O + SO_2$$

$$2H_2S + SO_2 \rightarrow 2H_2O + 3S$$

Kasumov[126] investigated the deactivation of alumina catalyst taken from different bed heights of an industrial Claus reactor, using as techniques XPS, IR spectroscopy, high-resolution EM, and activity tests for the Claus reaction. After 3 years of industrial use, the two uppermost layers of the catalyst were largely deactivated due to the formation and accumulation of amorphous aluminum sulfate in the outer shell of the catalyst granules. The two lower bed layers were deactivated to a lesser extent, their activity still being close to that of the fresh catalyst. Sulfate formation is also the cause of catalyst deactivation of iron oxide catalyst for the selective oxidation of H_2S to elemental sulfur in tail gas from the Claus process (van den Brink et al.[127]).

V. Vanadia-on-Titania Catalysts

Supported vanadia constitutes the most important type of catalysts for selective oxidation of hydrocarbons. Nikolov et al.[128] investigated the reasons for deactivation of a V_2O_5/TiO_2 catalyst for the oxidation of *o*-xylene to phthalic anhydride under industrial conditions. The catalytic activity and selectivity were tested in an integral pilot-plant reactor; the changes of the catalyst were studied by XRD, IR spectroscopy, EM, and other techniques. The catalyst deactivation was found to be due to at least three independent reasons: (a) anatase–rutile transformation, (b) decrease of specific surface area, and (c) decrease in surface concentration of the promoters P_2O_5 and WO_3. The decrease in activity results from a and b and that in selectivity from c.

W. Catalysts for Auto Exhaust Emission Control

When automotive catalysts were developed in the 1970s, they represented in many ways the frontiers of knowledge in catalysis at that time. In no other chemical process are the catalysts subjected to such extents of unsteady operation and process abuses as in auto-exhaust catalysts. During the 50 000-mile running of the automobile, using an *unleaded* gasoline, the few grams of noble metal in the catalyst have to suffer the passage over the catalyst of 8 g of Pb, 1500 g of S, a few grams each of P, Cl, and Br, 200–500 g of Mn (from octane boosters containing Mn), etc., from the gasoline, while the engine oil contributes 50 g of Zn, 54 g of P, 145 g of S, 120 g of Ba, 200 g of Ca, 75 g of Mg, 8 g of B, and 540 g of ash and the construction materials their own metallic poisons like Cu, Zn, Fe, and Cr (see Shelef et al.[129]).

Stenbom et al.[130] studied the thermal deactivation of a commercial Pt–Rh three-way auto-exhaust catalyst at 950 °C for 24 h in dry N_2 with 2% O_2. The performance of the fresh and aged catalyst samples was characterized using a synthetic exhaust-flow system. For CO, hydrocarbons, and NO_x, the light-off temperature (the temperature required to give 50% conversion) on the aged sample was 70 °C higher than that for the fresh one. The effect of aging on steady-state performance at higher temperatures (>400 °C) was more moderate. The two catalyst samples were characterized by electron microscopy (TEM/SEM/EDS), XPS, and XRD; the total precious-metal (Pt + Rh) dispersion was determined by CO chemisorption and the total surface area by the BET method. TEM pictures show that the metal particles containing Pt and Rh had an average diameter of 3–4 nm in the fresh sample (Figure 24). In the used catalyst, very large sintered Pt particles could be seen: 100–300 nm size in TEM, as shown in Figure 25, while SEM showed occasionally even enormously large (a few microns in size!) plate-like precious-metal particles of the type shown in Figure 26. The Pt/Rh ratio was 12 on the sintered particle, compared to 5.5 on the fresh one, suggesting more Pt in the sintered particles. XPS measurements showed a higher degree of Rh oxidation in the aged sample. XRD did not indicate any phase transition of the support to α-alumina. The total (Pt + Rh) precious-metal dispersion values, determined from CO chemisorption and from TEM, were 0.25 and 0.25–0.30 for the fresh catalyst and 0.06 and 0.01 for the aged catalyst, respectively. The dispersion ratio (fresh catalyst)/(aged catalyst) is 4 from CO chemisorption and 30 from TEM; these ratios may be

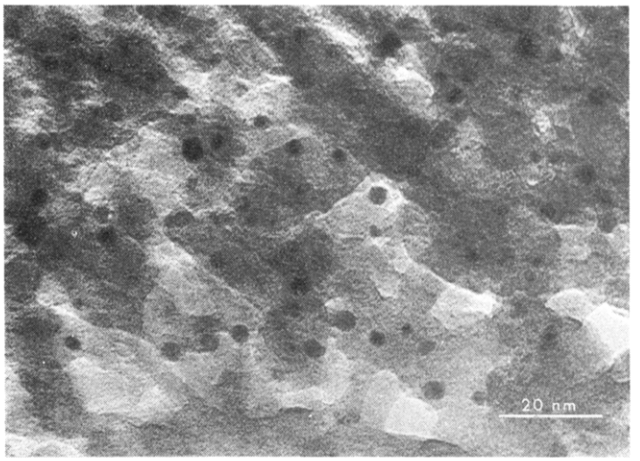

Figure 24. Transmission electron micrograph of fresh Pt–Rh/alumina three-way auto exhaust catalyst, showing uniform distribution of precious-metal particles (from Stenbom et al.,[130] reprinted with permission from 900273, copyright 1990 Society of Automotive Engineers).

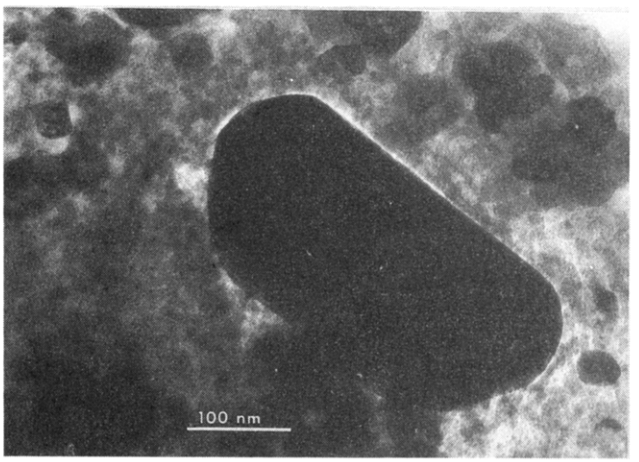

Figure 25. Transmission electron micrograph of the aged Pt–Rh/alumina catalyst, showing a large sintered precious-metal particle (cf. Figure 24 for contrast) (from Stenbom et al.,[130] reprinted with permission from 900273, copyright 1990 Society of Automotive Engineers).

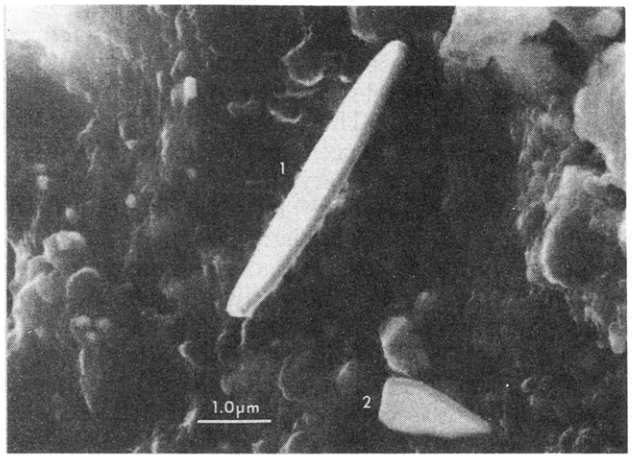

Figure 26. Scanning electron micrograph of the same aged catalyst as in Figure 25, showing two enormously large and plate-like precious-metal particles, marked 1 and 2, of a few microns in size (from Stenbom et al.[130] reprinted with permission from 900273, copyright 1990 Society of Automotive Engineers).

compared to the ratio of 12 for the number of active sites in the fresh/aged catalyst, derived from the Arrhenius plot of the CO-conversion data.

The catalysts used for emission control from gas turbines do not fare any better than auto-exhaust catalysts as far as the accumulation of impurities from the fuel is concerned. After 2 years of continuous operation, such catalysts typically show (Jung and Becker[131]) an impurity/poison accumulation on them of 1.8 wt % Fe, 1.3% Na, 1.0% S, and 1.0% As. The surface area of the catalyst had dropped from its original 150 m^2/g to 80 m^2/g and the catalyst surface was covered to a great extent with very fine iron oxide particles of 40–200 nm in size.

The catalysts for controlling emissions from automobiles and gas turbines have been carefully designed to withstand all the rigours of *normal* operations and poison levels in the fuel. Still, these catalysts may be prematurely deactivated if their operating conditions are beyond their design specifications.

X. Selective Catalytic Reduction of NO_x

For elimination of NO_x from industrial flue gases, selective catalytic reduction (SCR) has become the major present-day technology (cf. Bosch and Janssen[132]). Tokarz et al.[133] have studied flue gases from a municipal waste-incineration plant and the different elements in the form of their oxides emanating therefrom to determine their influence on a $V_2O_5/TiO_2/SiO_2$-type of SCR de-NO_x catalyst. These elements were found to be present on the surface of the catalyst after exposure to flue gases for 2000 h (Table 9). Hence their influence could be studied by their deliberate addition either separately or in gas mixtures. Changes in NO_x conversion, NH_3 slip, and BET surface area were measured in such artificial poisoning experiments. Tokarz et al. conclude that (1) at least 10 elements were detected on the surface of used catalysts (see Table 9); (2) activity of the catalyst is not affected by the quantity of elements on its surface beyond 2000 h; (3) of the elements present on the surface, Mg, K, and Na have the highest negative effects on catalyst performance; Fe, Al, Ca, and Zn have a moderate effect; and Ni, Ba and Cr have little or no effect; (4) experiments

Table 9. Concentration of Elements Deposited on the Samples of a De-NO_x Catalyst, Allowed To Age in the Flue-Gas Stream of a Municipal Waste Incineration Plant in Sweden[a] (from Tokarz et al.,[133] Copyright 1991 Elsevier)

compound	sample after 1840 h	sample after 2280 h	element	sample after 1840 h	sample after 2280 h
Fe_2O_3 (%)	0.20	0.42	Ba (ppm)	26	10
Al_2O_3	0.08	0.17	Cr	56	296
MgO	0.03	0.03	Cu	10	23
CaO	0.22	0.17	Ni	42	182
K_2O	0.02	0.08	Pb	90	90
Na_2O	0.03	0.21	Sr	7	4
P_2O_5	0.02	0.05	Zn	1200	1100
			Zr	310	570
			NO_x conversion (%)	90.5	90.5

[a] Samples were analyzed using inductive coupled plasma spectroscopy. Trace amounts of other metals such as Be, Co, La, Li, Sc, Y, and Mn were also detected.

using a mixture of 10 elements and simulating the aging effect for long periods up to 50 000 h at 180 °C suggest that the catalyst should remain active (NO_x conversion >80%) for at least 2 years in commercial operation. See also the chapter on "Deactivation of stationary source air emission control catalysts" by Kittrell et al. in ref 16.

Y. Elimination of VOC by Catalytic Combustion

Catalytic combustion, as an alternative to conventional thermal combustion, has received considerable attention in recent years. The introduction of solid catalysts into a traditionally noncatalytic free-radical process like combustion is a result of pressures from two areas: (1) the energy crisis and the resulting need to enhance the thermal efficiency of anything burned and (2) the legislations to reduce harmful emissions such as NO_x into the atmosphere. The major applications of catalytic combustion are two-fold: low-temperature catalytic combustion, already developed, to eliminate the emission into air of volatile organic chemicals (VOC) and high-temperature catalytic combustion, still under development, to enhance fuel efficiency and reduce NO_x emissions from gas turbines, jet motors, etc. These two aspects will be dealt with in this and the following section.

Catalytic combustion is a practical method to eliminate traces of VOC of a toxic nature or of an offensive odor, present in air from working spaces, purge or vent gas streams in industries, etc. Spivey and Butt[134] reviewed this area comprehensively in 1992. Agarwal et al.[135] studied the deactivation of chromia–alumina catalyst, used for oxidation of VOC in both fixed and fluidized bed reactors. The deactivation runs on fixed-bed reactors were terminated after 150 days on stream. The color of the catalyst bed had changed to green at the top one-third of the bed and to green-brown in the middle, while the lowest one-third had still the original brown color. XPS analysis showed an increase in the Cr-2p binding energy from the outlet to the inlet of the bed. Apparently chromium oxide was being converted to a higher oxidation state or forming chromium oxychlorides (chlorine from the traces of chlorinated hydrocarbons in the feed). As the front part of the bed is deactivated, the reaction zone moves down until the bed exit is reached, when the total conversion will decrease rapidly. Of course, such a color change could

not be observed in the fluidized bed because of the constant motion of the particles.

Z. High-Temperature Catalytic Combustion

In suppressing emissions of nitrogen oxides (NO_x) into the atmosphere, high-temperature oxidation/combustion catalysts have a very important role to play. A major part of NO_x emissions is from the so-called thermal NO_x, formed by oxidation of atmospheric nitrogen. The formation of thermal NO_x increases exponentially with temperature, but it does not become significant below 1200–1300 °C under gas-turbine burner conditions. In gas-turbine burners, peak temperatures can be up to 1800–2000 °C. The hot gases are then diluted with cold air to obtain a suitable temperature for the turbine inlet. The introduction of a catalyst allows complete combustion at much lower temperatures (leaner mixtures), avoiding emissions of CO and unburned fuel. The lowering of flame temperature by 200–300 °C practically eliminates the thermal formation of NO_x. This, in turn, makes it unnecessary to have expensive downstream de-NO_x facilities like scrubbers or large reactors for selective catalytic reduction of NO_x. Catalytic combustion is thus a *preventive* solution to the NO_x problem.

Particular interest in high-temperature applications of catalytic combustion, such as for gas turbines, has evolved during recent years.[136–139] In this case, catalyst temperatures will have to be in the range of 1100–1400 °C for sustained operation for 8000 h or 1 year. Conventional oxidation or combustion catalysts like noble metals or transition-metal oxides are not resistant to such severe operating conditions; they also do not have the necessary thermal-shock resistance. Hence novel materials like La-based perovskites, $LaBO_3$, and $LaCoO_3$ and barium hexaaluminates, $BaO{\cdot}6Al_2O_3$, are being developed to serve as catalyst and support which can withstand high temperatures in atmospheres containing steam and oxygen. Under such conditions, catalyst poisoning of the ordinary type is not important anymore, because the poisons volatilize off readily. On the other hand, new complications arise: chemical reactions between the support and the catalytic components, thermal and hydrothermal stability of the various solid-state phases, mechanical strength, etc. The high-volume throughput also makes it imperative that only honeycomblike monolithic structures for the catalyst will ensure sufficiently low pressure drop.

A typical example of the unusual and very subtle problems encountered in developing catalysts for high-temperature catalytic combustion is given in a very recent study[140] by the Kyushu University (Kyushu, Japan) group of Arai, who pioneered the work on substituted hexaaluminates as catalytic materials.[141] The catalytic properties of Pd supported on hexaaluminates ($Sr_{0.8}La_{0.2}XAl_{11}O_{19}$, where X = Al and Mn) were studied[141] for use in high-temperature catalytic combustion. The activity of the supported Pd catalyst increased initially with a rise in temperature, but decreased at higher temperatures (about 700 °C). The drop in catalytic activity became pronounced when the supported Pd particles were sintered into large agglomerates after calcination above 1000 °C. From *in situ* XRD and temperature-programmed desorption (TPD) and oxidation (TPO), it was revealed that the activity drop accompanies a dissociation of PdO onto metallic Pd species. Since the dissociation of PdO is thermodynamically dependent on oxygen partial pressure, the temperature at which the conversion drop appeared is influenced by the oxygen concentration in the fuel–air mixture. The dissociation of PdO seems to remove adsorbed oxygen species necessary for the catalytic combustion. Very similar results were also obtained by Ferrauto et al.[142] from a study of the high-temperature catalytic chemistry of supported Pd for combustion of methane. Palladium oxide supported on alumina decomposes in two distinct steps in air at atmospheric pressure. The first step occurs between 750 and 800 °C and is believed to be a decomposition of Pd–O species dispersed on bulk Pd metal, designated (PdO_x/Pd). The second decomposition occurs between 800 and 850 °C and it behaves like crystalline palladium oxide (PdO). To form the oxide once again, metallic Pd has to be cooled down to 650 °C, thus causing a hysterisis gap of 150 °C. Above 500 °C, catalytic methane oxidation can occur only as long as the palladium oxide phase is still present. Above 650 °C, metallic Pd cannot chemisorb oxygen and hence it is catalytically inactive toward methane oxidation.

A significant drop in catalytic activity for catalytic combustion of methane due to the above-mentioned PdO decomposition or the inability of metallic Pd to chemisorb oxygen above 650 °C, however, can be effectively avoided by using a catalytically more active Mn-substituted hexaaluminate (X = Mn) as a catalyst support (Sekizawa et al.[140]). The catalytic activity of this magnesium hexaaluminate compensates for the drop in activity of Pd so that a stable combustion reaction can be attained in a whole temperature range. Thus, the use of *catalytically active support materials* is one possible solution to overcome the unstable activity of the supported Pd catalyst in high-temperature combustion. This is an area of research where the terms active catalyst, catalyst support, and promoter have no longer their conventional meaning.

Since none of the catalytic materials available today can fulfill all the requirements of high-temperature and sufficiently long-term operation, system engineering is being suitably adapted to overcome the intrinsic limitations of the catalytic materials. Thus, hybrid catalytic/thermal combustors and multiple-monolith catalyst systems are being tried; each one is kept and operated in its own "safe zone" so that damage to the catalyst can be minimized. These and other developments in catalytic materials for high-temperature combustion were covered in a review by Zwinkels et al.[143] in 1993.

IV. Concluding Remarks

During the last few decades, an increasing number of powerful surface characterization techniques have become available to examine what happens *on* the surface or *to* the surface of solid catalysts. These techniques, mostly in combination, can be applied to follow the changes of a catalyst from its fresh or unused state to its active/equilibrium state under process conditions and later to its deactivated state. Understanding such transformations of the catalyst at the atomic/molecular level is important for several reasons: for the advancement of catalysis as a science, for trouble-shooting in the plant, for a better utilization of the present-day catalysts in the existing plants, and for

the design of still better and more rugged catalysts to meet the increasing demands of energy-related pressures and environmental legislations.

Recent work on catalysts for ammonia synthesis, methanol synthesis, fluid catalytic cracking, dehydrogenation of ethyl benzene to styrene, ammoxidation of propylene to acrylonitrile, hydrotreating, auto exhaust emission control, etc., shows that many modern surface-science techniques can be used to study practical catalysts from industry, if these catalysts are taken directly into the high-vacuum or ultrahigh vacuum chamber. This is in refreshing contrast to the hitherto often prevalent (perhaps mistaken?) belief or attitude that such techniques are suitable only for fundamental surface-science work on ideal solid surfaces under UHV conditions, very remote from the real world of industrial catalysis. This new "bridge" between fundamental and applied catalysis is very timely and essential. The possibility to conduct *in situ* time-resolved measurements is adding a new dimension to such characterization studies.

It should be emphasized, however, that it is just the combination of classical surface-characterization techniques with the more recent physical techniques which has resulted in most of the progress mentioned above. At the same time, it is also important to be aware of typical methodological problems which are inherent to the various techniques being used: for instance, what one can expect from techniques like XPS or UPS and what is beyond their possibilities? This problem has just been highlighted in a series of papers by Muhler et al.,[144] Paál and Schlögl,[145] and Paál et al.[146,147] It is sobering indeed to realize that even a "regenerated" Pt surface cannot be regarded as carbon-free or that a reduction treatment does not remove all oxygen from a Pt surface, since a considerable amount of H_2O/OH can still be present on this surface.[145]

Refinements in catalysts often lead to improvements in catalytic processes and engineering. Conversely, high-temperature catalytic combustion is a fascinating area to demonstrate how systems engineering can be called in for a rescue operation of the catalyst, when the material aspects of the catalyst have still not reached maturity for the extremely demanding operating conditions (cf. Zwinkels et al.[143]).

Catalysis R&D can be justifiably proud of several successes in all these areas in recent times.

V. Acknowledgments

The author thanks Prof. Gabor A. Somorjai who first proposed the writing of this review for *Chemical Reviews*. Special thanks are due to Prof. Gilbert F. Froment for fruitful collaboration in research in his Laboratory at the University of Gent over two long periods and for his valuable comments on the draft manuscript of this review. The author is highly indebted to Professors Nils-Herman Schöön, Jan-Erik Otterstedt, and Leif Holmlid (all at the Chalmers University of Technology, Göteborg, Sweden) and Sven Järås (first at EKA-Nobel and later at the Royal Institute of Technology, Stockholm, Sweden), colleagues and friends who made the author's "Swedish contacts" so important and pleasant for him during the last 15 years. A critical reading of the manuscript by the author's former colleagues, Dr. Frits van Buren and Dr. Domien van Oeffelen (both of Dow Chemical, Terneuzen, The Netherlands), and by Dr. David Lafyatis has helped in smoothening some of its sharp corners. Financial support from the Swedish Board for Technical Development (STU/NUTEK) from 1984 onward is gratefully acknowledged.

VI. References

(1) Gibbs, J. W. *Trans. Conn. Acad. Arts Sci.* **1875/76**, *3*, 108; **1877/78**, *5*, 343.
(2) Overbury, S. H.; Bertrand, P. A.; Somorjai, G. A. *Chem. Rev.* **1975**, *75*, 547.
(3) Ponec, V. *Catal. Rev.—Sci. Eng.* **1975**, *11*, 41.
(4) Sachtler, W. M. H. *Catal. Rev.—Sci. Eng.* **1976**, *14*, 193.
(5) Sachtler, W. M. H.; van Santen, R. A. *Advan. Catal.* **1977**, *26*, 69.
(6) Somorjai, G. A. *Chemistry in Two Dimensions: Surfaces*; Cornell University Press: Ithaca, NY, 1881.
(7) Menon, P. G.; Prasada Rao, T. S. R. *Catal. Rev.—Sci. Eng.* **1979**, *20*, 97–120.
(8) Anderson, R. B., Ed. *Experimental Methods in Catalytic Research*, Vol. 1, 1968; Vol. 2, 1972; Vol. 3, 1976; Academic Press: New York.
(9) Kane, P. F.; Larrabee, G. B., Eds., *Characterization of Solid Surfaces*, Plenum Press: New York, 1974.
(10) Thomas, J. M.; Lambert, R. M. *Characterization of Catalysts*; John Wiley & Sons: Chichester, UK, 1980.
(11) Delannay, F., Ed. *Characterization of Heterogeneous Catalysts*; Marcel Dekker: New York, 1984.
(12) Srivastava, R. D. *Heterogeneous Catalytic Science*; CRC Press, Boca Raton, FL, 1988.
(13) Brongersma, H. H.; van Santen, R. A., Eds. *Fundamental Aspects of Heterogeneous Catalysis Studied by Particle Beams*; Plenum Press: New York, 1991.
(14) Wachs, I. E., Ed., *Characterization of Catalytic Materials*; Butterworth: Oxford, 1993.
(15) Niemantsverdriet, J. W. *Spectroscopy in Catalysis: An Introduction*; VCH: Weinheim (Germany), 1993.
(16) Spivey, J. J., Ed. *Catalysis*; Specialist Periodical Report; Royal Soc. Chem.: London, 1992; Vol. 9.
(17) Austermann, R. L.; Denley, D. R.; Hart, D. W.; Himelfarb, P. B.; Irwin, R. M.; Narayana, M.; Szentirmay, R.; Tang, S. C.; Yeates, R. C. *Anal. Chem.* **1987**, *59*, 68R–102R.
(18) Menon, P. G. in ref 29, pp 99–123. Menon, P. G. In *Hydrogen Effects in Catalysis—Fundamentals and Practical Applications*; Paál, Z., Menon, P. G., Eds.; Marcel Dekker: New York, 1988; pp 117–138.
(19) Menon, P. G. *Catal. Today* **1991**, *11*, 161–172.
(20) Bradley, S. A., Gattuso, M. J., Bertolacini, R. J., Eds. *Characterization and Catalyst Development: An Interactive Approach*; ACS Symposium Series 411; American Chemical Society: Washington, DC, 1989.
(21) Barr, T. L. *Appl. Surf. Sci.* **1983**, *15*, 1.
(22) Barr, T. L.; Chen. L. M.; Mohsenian, M.; Lishka, M. A. *J. Am. Chem. Soc.* **1988**, *110*, 7962.
(23) Barr, T. L. In *Practical Surface Analysis*, 2nd ed.; Briggs, D., Seah, M. P., Eds.; John Wiley; Chichester, U.K., 1990; Chapter 8.
(24) Barr, T. L.; Lishka, M. A. *J. Am. Chem. Soc.* **1986**, *108*, 3178.
(25) Barr, T. L. *Crit. Rev. Anal. Chem.* **1991**, *22*, 229.
(26) Barr, T. L. *Zeolites* **1990**, *10*, 760.
(27) Barr, T. L. *Crit. Rev. Anal. Chem.* **1991**, *22*, 113.
(28) Delmon, B., Froment, G. F., Eds. *Catalyst Deactivation* (1980); Elsevier: Amsterdam, 1980.
(29) Petersen, E. E., Bell, A. T., Eds. *Catalyst Deactivation* (1985); Marcel Dekker: New York, 1987.
(30) Delmon, B.; Froment, G. F., Eds. *Catalyst Deactivation 1987*; Elsevier: Amsterdam, 1987.
(31) Bartholomew, C. H.; Butt, J. B., Eds. *Catalyst Deactivation 1991*; Elsevier: Amsterdam, 1991.
(32) Delmon, B.; Froment, G. F., Eds. *Catalyst Deactivation 1994*; Elsevier: Amsterdam, 1994.
(33) Froment, G. F. *Proceedings of the 6th International Congress on Catalysis, London*; Chemical Society: London, 1976; p 10.
(34) Froment, G. F. In ref 28, p 1.
(35) Menon, P. G. *J. Mol. Catal.* **1990**, *59* (1990) 207–220.
(36) Maxted, E. B. *Adv. Catal.* **1951**, *3*, 129.
(37) Hegedus, L. L.; McCabe, R. W. *Catal. Rev.—Sci. Eng.* **1981**, *23*, 377; *Catalyst Poisoning*, Marcel Dekker: New York, 1984.
(38) Butt, J. B.; Petersen, E. E. *Activation, Deactivation, and Poisoning of Catalysts*, Academic Press: New York, 1988.
(39) Oudar, J.; Wise, H., Eds. *Deactivation and Poisoning of Catalysts*; Marcel Dekker: New York, 1985.
(40) Ruckenstein, E.; Sushumna, I. In *Hydrogen Effects in Catalysis: Fundamentals and Practical Applications*; Paál, Z., Menon, P. G., Eds.; Marcel Dekker: New York, 1988, pp 259–291.
(41) Ruckenstein, E. In ref 31, p 585.
(42) Lee, W. H.; Petrova, V.; van Loon, K. R.; Woodhouse, J. B.; Loxton, C. M.; Finnegan, N. L.; Masel, R. I. In ref 31, p 597.
(43) Haber, J. in Ruiz, P.; Delmon, B., Eds. *Studies in Surface Science & Catalysis*, 1992; Elsevier: Amsterdam; Vol. 72, p 279–304.
(44) Xie, Y.-C.; Tang, Y.-Q. *Adv. Catal.* **1990**, *37*, 1–43.
(45) Burch, R. in Paál, Z.; Menon, P. G. (Eds.) *Hydrogen Effects in Catalysis—Fundamentals and Practical Applications*; Marcel Dekker: New York, 1988; p 347–372.

(46) Mahdi, W.; Schütze, J.; Weinberg, G.; Schoonmaker, R.; Schlögl, R.; Ertl, G. *Catal. Lett.* **1991**, *11*, 19–32.
(47) Arunarkavalli, T.; Kulkarni, G. U.; Rao, C. N. R. *Catal. Lett.* **1993**, *20*, 259–268.
(48) Duprez, D.; Ferhat-Hamida, Z.; Bettahar, M. M. *J. Catal.* **1990**, *124*, 1.
(49) Couves, J. W.; Thomas, J. M.; Waller, D.; Jones, R. H.; Dent, A. J.; Derbyshire, G. E.; Greaves, G. N. *Nature* **1991**, *354*, 465.
(50) Amiridis, M. D.; Pugliri, F.; Dumesic, J. A.; Millman, W. S.; Topsoe, N-Y. *J. Catal.* **1993**, *142*, 572; see also Clausen, B. S.; Grabaek, L.; Hansen, P. L.; Steffensen, G.; Topsoe, H. Paper presented at the First European Conference on Catalysis, Montpellier, Sept 13–17, 1993.
(51) Rao, C. N. R.; Kulkarni, G. V.; Kannan, K. R.; Chaturvedi, S. *J. Phys. Chem.* **1992**, *96*, 7379.
(52) Muhler, M.; Schlögl, R.; Ertl, G. *J. Catal.* **1992**, *138*, 413.
(53) Herzog, B.; Bensch, W.; Ilkenhaus, Th.; Schlögl, R. *Catal. Lett.* **1993**, *20*, 203.
(54) Twigg, M. V., Ed. *Catalyst Handbook*; Wolfe Publishing: London, 1989.
(55) Jennings, J. R., Ed. *Catalytic Ammonia Synthesis—Fundamentals and Practice*, Plenum Press: New York, 1991.
(56) Emmett, P. H.; Brunauer, S. *J. Am. Chem. Soc.* **1937**, *59*, 210. Brunauer, S.; Emmett, P. H. *J. Am. Chem. Soc.* **1940**, *62*, 1732.
(57) Silverman, D. C.; Boudart, M. *J. Catal.* **1982**, *77*, 208.
(58) Davis, S. M. *Catal. Lett.* **1988**, *1*, 85.
(59) Spencer, M. S. In ref 54, pp 71.
(60) Knez, S.; Shires, S.; Tennison, S. *Proceedings of the 8th International Symposium on Large Chemical Plants*, Antwerp, Oct 12–14, 1992, pp 129–139.
(61) Chang, C. D. *Catal. Rev.—Sci. Eng.* **1983**, *25*, 1; *Hydrocarbons from Methanol*; Marcel Dekker: New York, 1983.
(62) Wender, I. *Catal. Rev.*—Sci. *Eng.* **1984**, *26*, 303.
(63) Bridger, G. W.; Spencer, M. S. In ref 54, pp 441–468.
(64) Tonner, S. P.; Wainwright, M. S.; Trimm, D. L.; Cant, N. W. *Appl. Catal.* **1983**, *18*, 215.
(65) Evans, J. W.; Casey, P. S.; Wainwright, M. S.; Trimm, D. L. *Appl. Catal.* **1983**, *7*, 31.
(66) Onsager, O. T. Canadian Patent 1,175,798, 1984.
(67) Onsager, O. T.; Wittgens, B.; Saraker, P. *VI International Symposium on the Relation between Homogeneous and Heterogeneous Catalysis*, Pisa, Italy; Sept 25–29, 1989, p 112.
(68) Liu, Z.; Tierney, J. W.; Shah, Y. T.; Wender, I. *Fuel Process. Tech.* **1988**, *18*, 185.
(69) Palekar, V. M.; Jung, H.; Tierney, J. W.; Wender, I. *Appl. Catal.* **1993**, *102*, 13.
(70) Haensel, V.; Haensel, H. S. Paper in ref 20, p 2–11.
(71) Menon, P. G.; Prasad, J. *Proceedings of the 6th International Congress Catalysis*; Chemical Society: London, 1976, Vol. 2, pp 1061–1071.
(72) Menon, P. G.; Marin, G. B.; Froment, G. F. *Ind. Eng. Chem., Prod. Res. Dev.* **1982**, *21*, 52.
(73) Bickle, G. M.; Beltramini, J. N.; Do, D. D. *Ind. Eng. Chem. Res.* **1990**, *29*, 1801.
(74) Rostrup-Nielsen, J. R. *Steam Reforming Catalysts*; Teknisk Forlag: Copenhagen, 1975.
(75) De Deken, J.; Menon, P. G.; Froment, G. F.; Haemers, G. *J. Catal.* **1981**, *70*, 225.
(76) Hoste, S.; van der Vondel, D.; van der Kelen, G. P.; de Deken, J. *J. Electron Spectr.* **1979**, *16*, 407.
(77) Boitiaux, J. P.; Cosyns, J.; Verna, F., in ref 30, p 106.
(78) Dalla Betta, R. A.; Boudart, M. *Proceedings of the 5th International Congress on Catalysis*; 1972, Vol. 2, p 1329.
(79) Palczewska, W. in Paál, Z.; Menon, P. G. (Eds.) *Hydrogen Effects in Catalysis—Fundamentals and Practical Applications*; Marcel Dekker: New York, 1988; p 373–395.
(80) Bhasin, M. M. *J. Catal.* **1975**, *38*, 218.
(81) Couvillion, M. C. U.S. Patent 4,440,956, 1984; *Chem. Abstr.* **1984**, *100*, 216459n.
(82) Couvillion, M. C. U.S. Patent 4,493,906, 1985; *Chem. Abstr.* **1985**, *102*, 101286c.
(83) Menon, P. G. Unpublished results from 1989–90.
(84) Prasada Rao, T. S. R. Personal communication (1981).
(85) Otterstedt, J. E.; Gevert, B.; Menon, P. G.; Järås, S. *Appl. Catal.* **1986**, *22*, 159–179.
(86) Biswas, J.; Maxwell, I. *Appl. Catal.* **1990**, *63*, 197–258.
(87) Järås, S. *Appl. Catal.* **1982**, *2*, 207.
(88) Leta, L. P.; Kugler, E. L. Paper in ref 1, p 354.
(89) Andersson, S. L. T.; Lundin, S. T.; Järås, S.; Otterstedt, J. E. *Applied Catal.* **1984**, *9*, 317.
(90) Pompe, R.; Järås, S.; Vannerberg, N. G. *Applied Catal.* **1984**, *13*, 171.
(91) Occelli, M. L., Ed., *Fluid Catalytic Cracking: Role in Modern Refining*; ACS Symp. Series 375; American Chemical Society: Washington, DC, 1988.
(92) Lee, E. H. *Catal. Rev.* **1973**, *8*, 285.
(93) Mross, W. D. *Catal. Rev.—Sci. Eng.* **1983**, *25*, 17.
(94) Connell, C.; Dumesic, J. A. *J. Catal.* **1985**, *82*, 17.
(95) Muhler, M.; Schutze, J.; Wesemann, M.; Rayment, T.; Dent, A.; Shlögl, R.; Ertl, G. *J. Catal.* **1990**, *126*, 339.
(96) Büchele, W. Lecture at the 2nd Paul Sabatier Conference on Catalysis, Strasbourg, September 1991.
(97) Stobbe, D. E. Ph.D. Thesis, University of Utrecht, 1990.
(98) Stobbe, D. E.; van Buren, F. R.; Orbons, A. J.; van Dillen, A. J.; Geus, J. W. *J. Mater. Sci.* **1992**, *27*, 343.
(99) Stobbe, D. E.; van Buren, F. R.; Stobbe-Kreemers, A. W.; Schokker, J. J.; van Dillen, A. J.; Geus, J. W. *J. Chem. Soc., Faraday Trans.* **1991**, *87* (10), 1623.
(100) Stobbe, D. E.; van Buren, F. R.; Hoogenraad, M. S.; van Dillen; Geus, J. W. *J. Chem. Soc., Faraday Trans.* **1991**, *87* (10), 1639.
(101) Stobbe, D. E.; van Buren, F. R.; van Dillen, A. J.; Geus, J. W. (a) *J. Catal.* **1991**, *135*, 533; (b) *J. Catal.* **1991**, *135*, 548; (c) in *Proceedings of the 10th International Congress on Catalysis, Budapest*, 1992, Part C, Guczi et al., Ed., Elsevier Science Publ.: Amsterdam, 1993, p 2337.
(102) Hirano, T. *Bull. Chem. Soc. Jpn.* **1986**, *59*, 2672; *Appl. Catal.* **1986**, *26*, 65; **1986**, *28*, 119.
(103) Lundin, J.; Engvall, K.; Holmlid, L.; Menon, P. G. *Catal. Lett.* **1990**, *6*, 85; Lundin, J., Ph.D. Thesis, Göteborg, 1993.
(104) Engvall, K.; Holmlid, L.; Menon, P. G. *Appl. Catal.* **1991**, *77*, 235; Engvall, K. Ph.D. Thesis, Göteborg, 1994.
(105) Holmlid, L.; Engvall, K.; Åman, C.; Menon, P. G. In ref 101c, p 795.
(106) Åman, C.; Holmlid, L. *Appl. Surface Sci.* **1992**, *62*, 201; **1993**, *64*, 71.
(107) Lundin, J.; Holmlid, L.; Menon, P. G.; Nyborg, L. *Ind. Eng. Chem. Res.* **1993**, *32*, 2500.
(108) Prasada Rao, T. S. R.; Menon, P. G. *J. Catal.* **1978**, *51*, 64.
(109) Xiong, Y. L.; Castillo, R.; Papadopoulou, Ch.; Daza, L.; Ladriere, J.; Ruiz, P.; Delmon, B. In ref 31, p 425.
(110) Delmon, B. *Bull. Soc. Chim. Belg.* **1979**, *16*, 473–476; *C. R. Acad. Sci. Paris* **1979**, *289 ser. C*, 173–176; *Int. Chem. Eng.* **1980**, *20*, 639–641; *React. Kinet. Catal. Lett.* **1980**, *13*, 203–208.
(111) Lee, J. C.; Trimm, D. L.; Wainwright, M. S.; Cant, A. W.; Kohler, M. A.; Onouha, N. I., In ref 30, p 235.
(112) Dvorak, B.; Pasek, J.; Pavlas, P.; Hejda, Z. In ref 30, p 535.
(113) Petrini, G.; Cesana, A.; De Alberti, G., Genoni, F.; Leofanti, G.; Padovan, M.; Paparatto, G.; Roffia, P. In ref 31, p 761.
(114) Arena, B. J. *Appl. Catal. A Gen.* **1992**, *87*, 219.
(115) Simpson, H. D. In ref 31, p 265.
(116) Ramaswamy, A. V.; Sharma, L. D. In ref 31, p 707.
(117) Clark, F. T.; Hensley, A. L.; Shyu, J. Z.; Kaduk, J. A.; Ray, G. J. In ref 31, p 417.
(118) Phillips, M. D.; Eastman, A. D. *Catal. Lett.* **1992**, *13*, 157.
(119) Mirodatos, C.; Perrichon, V.; Durupty, M. C.; Moral, P. In ref 30, p 183.
(120) Anderson, R. B. *The Fischer–Tropsch Synthesis*, Academic Press: New York, 1984.
(121) Dry, M. E.; Hogendoorn, J. C. *Catal. Rev.—Sci. Eng.* **1981**, *23*, 265.
(122) Dry, M. E. *Catal. Today* **1990**, *6*, 183–206.
(123) Dry, M. E. In *Catalysis Science and Technology*, Anderson, J. R., Boudart, M., Eds., Springer Verlag: New York, 1981, Vol. 1, pp 159–255.
(124) Xu, X.; Scholten, J. J. F. *Appl. Catal. A Gen.* **1992**, *82*, 91.
(125) Horner, B. T. *Platinum Metals Rev.* **1993**, *37*, 76–85.
(126) Kasumov, F. B. In ref 31, p 493.
(127) van den Brink, P. J.; Scholten, A.; van Dillen, A. J.; Geus, J. W.; Boellard, A. M.; van der Kraan, A. M. In ref 31, p 515.
(128) Nikolov, V. A.; Klissurski, D. G.; Hadjiivanov, K. I. In ref 30, p 173.
(129) Shelef, M.; Otto, K.; Otto, N. C. *Adv. Catal.* **1978**, *27*, 311.
(130) Stenbom, B.; Smedler, G.; Nilsson, P. H.; Lundgren, S.; Wirmark, G. Paper in *SAE International Congress and Exposition, Detroit*, Feb. 26—March 2, 1990, SAE Technical Paper Series, 900273, pp 1–10.
(131) Jung, H. J.; Becker, E. R. *Platinum Metals Rev.* **1987**, *31*, 162.
(132) Bosch, H.; Janssen, F. *Catal. Today* **1987**, *2*, 369–531.
(133) Tokarz, M.; Järås, S.; Persson, B. In ref 31, p 523.
(134) Spivey, J. J.; Butt, J. B. *Catal. Today* **1992**, *11*, 465–500.
(135) Agarwal, S. K.; Spivey, J. J.; Howe, G. B.; Butt, J. B.; Marchand, E. In ref 31, p 475.
(136) Trimm, D. L. *Appl. Catal.* **1983**, *7*, 249–282.
(137) Prasad, R.; Kennedy, L. A.; Ruckenstein, E. *Catal. Rev.—Sci. Eng.* **1984**, *26*, 1–58.
(138) Weinberg, F. D. (Ed.) *Advanced Combustion Methods*; Academic Press: New York, 1986.
(139) Pfefferle, L. D.; Pfefferle, W. C. *Catal. Rev.—Sci. Eng.* **1987**, *29*, 219–267.
(140) Sekizawa, K.; Machida, M.; Eguchi, K.; Arai, H. *J. Catal.* **1993**, *142*, 655.
(141) Machida, M.; Eguchi, K.; Arai, H. *J. Catal.* **1987**, *103*, 385; *Bull. Chem. Soc. Japan* **1988**, *61*, 2659; *J. Catal.* **1989**, *120*, 377; **1990**, *123*, 477.
(142) Ferrauto, R. J.; Hobson, M. C.; Kennelly, T.; Waterman, E. M. *Appl. Catal. A: Gen.* **1992**, *81*, 227.
(143) Zwinkels, M. F. M.; Järås, S. G.; Menon, P. G.; Griffin, T. A. *Catal. Rev. Sci. Eng.* **1993**, *35*, 319–358.
(144) Muhler, M.; Paál, Z.; Schlögl, R. *Appl. Surf. Sci.* **1991**, *47*, 281.
(145) Paál, Z.; Schlögl, R. *Surf. Interface Anal.* **1992**, *19*, 524.
(146) Paál, Z.; Schlögl, R.; Ertl, G. *J. Chem. Soc. Faraday Trans.* **1992**, *88*, 1179; *Catal. Lett.* **1992**, *12*, 331.
(147) Paál, Z.; Muhler, M.; Schlögl, R. *J. Catal.* **1993**, *143*, 318.